Heliyon 10 (2024) e39121

Contents lists available at ScienceDirect

Heliyon

journal homepage: www.cell.com/heliyon

Research article

State-of-health estimation and classification of series-connected batteries by using deep learning based hybrid decision approach

Volkan Yamaçli

Computer Engineering Department, Faculty of Engineering, Mersin University, P.O. Box 33100, Mersin, Turkey

A R T I C L E I N F O

Keywords:
State of health
Remaining useful life
Series-connected lithium-ion batteries
Deep learning based estimation
Hybrid-classification

A B S T R A C T

In rechargeable battery control and operation, one of the primary obstacles is safety concerns where the battery degradation poses a significant factor. Therefore, in recent years, state-of-health assessment of lithium-ion batteries has become a noteworthy issue. On the other hand, it is challenging to ensure robustness and generalization because most state-of-health assessment techniques are implemented for a specific characteristic, operating situation, and battery material system. In most studies, health status of single cell batteries is assessed by using analytical or computer-aided deep learning methods. But, the state-of-health characteristics of series-connected battery systems should be also focused with advances of technology and usage, especially electric vehicles. This study presents a data-driven, deep learning-based hybrid decision approach for predicting the state-of-health of series-connected lithium-ion batteries with different characteristics. The paper consists of generating series-connected battery degradation dataset by using of some mostly used datasets. Also, by employing deep learning-based networks along with hybrid-classification aided by performance metrics, it is shown that estimating and predicting the state-of-health can be achieved not only by using sole deep-learning algorithms but also hybrid-classification techniques. The results demonstrate the high accuracy and simplicity of the proposed novel approach on datasets from Oxford University and Calce battery group. The best estimated mean squared error, root mean square error and mean-absolute percentage error values are not more than 0.0500, 0.2236 and 0.7065, respectively which shows the efficiency not only by accuracy but also error indicators. The results show that the proposed approach can be implemented in offline or online systems with best average accuracy of 98.33 % and classification time of 58 ms per sample.

1. Introduction

1.1. Background and Motivation

For the last decade, lithium-ion batteries (LIB) have been used in various industries such as consumer electronics, energy storage systems, renewable connected smart grids, electric cars and transportation due to easy applicability and better energy/power density compared to other battery types such as lead–acid batteries and nickel–hydrogen batteries [1]. Also, LIBs have trait of negligible memory which makes this type of batteries economically preferable with long-life and higher charge/discharge cycle number with predictable degradation rate. An increasing number of clean-energy vehicles powered by LIBs are contributing to the development of

E-mail address: vyamacli@mersin.edu.tr.

https://doi.org/10.1016/j.heliyon.2024.e39121
Received 13 August 2024; Received in revised form 16 September 2024; Accepted 8 October 2024
Available online 9 October 2024

electrified transportation as a means of reducing air pollution and achieving in order to provide carbon neutral airspace. In 2022, it was predicted that 515.9 GWh of power batteries deployed worldwide and according to data compiled between January and June of 2023, the installed capacity of power batteries for automobiles worldwide reached 304.3 GWh, signifying a 50.1 % increase in just one year [2]. As lithium-battery technology continues to advance, batteries exhibit a high specific energy density. The health of a battery system generally indicates the safety and reliability of the energy storage systems during operation [3]. Exclusively, the capacity of a battery/battery system degrades after long-term usage that causes permanent capacity loss that also affects battery voltage and therefore system stability. Capacity degradation is the main sign of aging batteries, and it has a big effect on battery usability. A battery's condition of health is typically determined by comparing its current capacity to its initial rated capacity [4]. The time-consuming and energy-wasting nature of traditional methods of capacity determination which involve lengthy cycles of charging and discharging becomes more and more infeasible as the number and capacity of lithium-ion batteries increase. As a result, techniques for quickly, precisely, and effectively estimating battery health are desperately needed.

For a battery management system to operate safely and extend battery life, predictive maintenance is a critical. In order to implement battery management systems for managing, controlling, and optimizing battery utilization extraction of battery charge or health state is necessary [5]. State-of-charge (SOC) and state-of-health (SOH) are the two most important parameters of LIBs. The ratio of a battery's accessible capacity to its maximum charge capacity is known as its state of charge (SOC) at any point throughout a certain charge-discharge cycle. As a result, the SOC provides an indication of the battery's capacity to power the gadget during the current cycle. The battery degrades with use, which is a complicated, nonlinear process including both internal and external elements [6]. Typically, battery health prognostics refer to the assessment of the state of health (SOH) and the forecast of the remaining useful life (RUL). SOH is typically defined as the ratio of the current capacity to the nominal capacity of a brand-new battery cell. The number of cycles left before the end of the service life is known as the RUL which usually indicated when the capacity defined SOH reaches about 70 %–80 % [7]. Accurately predicting such values can enhance battery management in a number of ways. It is also possible to discuss the financial element, since maintenance expenses will be lower if the breakdown is anticipated in advance. Longer battery cycles result in less strain on primary resources, which ultimately has a less environmental impact [8]. A report to the user providing a reliable assessment of the battery's state of health (SOH) and maintenance advice might be provided by factoring operating data like current, voltage, and temperature into the predictive models. However, predicting and managing the degradation and aging of a battery system which consists of series and/or parallel connected batteries are not easy [9] despite being vital operation for safety and environmental friendliness [10].

The commonplace strategy of lithium-ion battery degradation forecast is ordinarily partitioned into two main categories that are model-based approach [11] and data driven approach [8,12,13]. The comprehensive inner state information, be that as it may, is regularly troublesome to distinguish and collect for battery corruption demonstrating due to the profoundly complex chemical responses interior lithium-ion battery. The lithium-ion batteries are vulnerable working temperature, electronic circuit, stack and other natural components; in this manner, it is troublesome to set up an exact expectation demonstrate for lithium-ion battery corruption. The data-driven strategy has as of late drawn critical consideration in LIB degradation forecast investigate region. However, most data-driven strategies are centered on making short-time forecast for a same battery based on the verifiable information of the battery, few existing strategies can realize multi-battery expectation by utilizing information from multi-battery [14].

1.2. Literature review

In literature, analytical and empirical techniques are employed for battery status estimation for data-driven models, historical data that are simple to gather from sensors is used to directly calculate the SOH of the battery. These methods either use battery capacity data directly or derive features from sensor data to estimate the SOH. The number of charge-discharge cycles that a battery has left before its condition falls below a predetermined level is known as its remaining useable life, or RUL. In some earlier studies, there have been used analytical models for SOH prediction and estimation. In Ref. [15] Xu et al. proposed a state-space based extended Kalman filter (EKF) model for RUL prediction while [16] Hu et al. proposed moving horizon estimation by employing reduced-electrotechnical model. He et al. [17] used Bayesian monte-carlo method for LIB prognostics. Micea et al. [18] employed a second-order polynomial model for online SOH assessment. In Ref. [19] enhanced single particle and physics-based single particle [20] models are used for LIB modelling and estimation. Gauss-hermit [21] particle filter techniques are also used for battery capacity prediction. Also, polynomial model is implemented for successful SOH estimation of lithium-ion batteries [22]. Therewithal, some other entropy and decomposition based analytical or artificial intelligence methods such as multiscale permutation entropy and variational modal decomposition [23] can be employed for battery-state prediction such as state of charge of state of health, successfully.

Recently, machine learning (ML) and deep-learning (DL) techniques such as recurrent neural networks (RNN), hybrid neural networks (HNN), convolutional neural networks (CNN) and support vector machines (SVM) have been used and applied for battery status monitoring and prediction. Statistical and machine learning models are the two further classifications for data-driven approaches for battery SOH estimation [24]. The following four steps are often included in a data-driven battery SOH estimate method: feature extraction, model training, data collecting, and SOH estimation [25]. Numerous data-driven methods for estimating battery SOH have been proposed [26].

In [27], Ma et al. used a hybrid neural network with false nearest neighbours to predict the RUL of batteries. Also, another hybrid neural network approach is used to LIB SOH estimation [28]. Tagade et al. [29] used a deep Gaussian process regression (DGPR) approach to predict LIB health and degradation status. In Ref. [30], an RNN model for predicting SOH degradation in batteries utilizing current and voltage measurements was presented. In Ref. [31] Liu et al. used a sparse autoencoder-based DNN to determine RUL of membrane fuel cells. Also, Zhang et al. [32] used support vector machine error compensation model for SOH estimation. In Ref. [33],

the SOH estimation of LIB is obtained by using long-term short memory (LSTM) neural networks and discrete wavelet transform. In order to enhance the precision of the battery RUL forecast, Park et al. [34] merged an LSTM model with multichannel charging profiles. Lin et al. [35] used probability density function (PDF) for successful SOH estimation on different datasets. In Ref. [36], Venugopal et al. employed sequential DNN and linear-regression method for SOH estimation, successfully. Also, Kumari et al. used R110-BLSTM (bidirectional long-short term memory) for classifying and predicting the SOH of one of the mostly used battery dataset [37]. In order to estimate battery SOH, Zheng et al. [38] suggested a CNN–GRU model utilizing voltage and current measurement data. In Ref. [39], Myilsamy et al. employed LSTM, CNN and hybrid learning method (HLM) to achieve a successful SOH prediction. Oh et al. also used LSTM on the experimental dataset for SOH prediction on railway vehicles which presents of a great importance for security [40]. By taking into account the battery's discharge capacity, linearly interpolated discharge capacity, linearly interpolated temperature, discharge quantity, and discharge duration as primary characteristics, Ren et al. [41] employed a CNN–LSTM model to predict the RUL of the battery. Also, in Ref. [42] Zou et al. employed LSTM on mostly used datasets which achieved lower classification error compared to such studies. In Refs. [43–45], boosting ant-colony optimization (BACO), stacking-based ensemble learning model (SBEL) and long-short term memory back propagation (LSTM-BP) methods are used to predict SOH of the same dataset, respectively. Also, series-connected LIB pack is studied for SOH and RUL prediction using health indicator extraction based on the partial charging curve (HIEPCC) by Hu et al. [46]. In addition to LIBs, supercapacitors are also studied for management and SOH estimation by using different state-of-art techniques, successfully [47,48].

2. Research gap and contributions

There are only a few studies focused on SOH estimation of series-connected LIB in spite of increasing integration of LIB packs into all kinds of electronic equipments especially electric vehicles, in literature. Even though changing on size, architecture and capacity; it is known that most electrical vehicles use LIB packs [49]. Therefore, the assessment of SOH prediction of series-connected LIB packs is a must for future planning both for technical aspects and security concerns. Zhou et al. [50] used a differential voltage analysis method for online SOH estimation of series-connected batteries while [51] used cell inconsistency evaluation for series-connected battery health modelling. Also, Che et al. [52] employed a universal deep learning method for SOH prognostics for series-battery packs. Also, Lu et al. [53] and Xu et al. [54] studied on electric vehicle batteries based on vibration signal and lithium-ion batteries with combined multi model, respectively.

Moreover, through direct measurement of the characterisation parameters linked to battery degradation and SOH prediction, the ampere-hour measurement method can be used to measure the capacity, or impedance and open circuit voltage can be measured directly [55]. However, current measurement method is challenging to apply and mostly only appropriate for use in a laboratory setting while charge or discharge voltage measurement is easier and simple with low lost and simple systems. In this study the capacities of series-connected LIB packs are used along with charging voltage characteristics for an easy-to-use implementation.

In this paper, it is proposed a DL based CNN approach by using AlexNet [56], ResNet [57] and DarkNet [58] for series-connected LIB degradation and SOH prediction. The CNNs aforementioned, are highly capable networks that may be used in various kinds of classification problems in areas such as engineering, medical, agriculture, physics, life sciences and more. In order to use the proposed classification techniques, the features of input data should be visualized. Therefore, for this study, related LIB data is processed by using continuous wavelet transform (CWT) which is one of the most advantageous signal processing methods for detecting signal characteristics under varying frequency responses and feature extraction [59]. Also, an easy implementation of CWT and DL techniques are applied by using voltage characteristics for single and series-connected LIB systems. The performance of the proposed method has been tested on different types of LIB characteristic on series-connected generated data using real measurement datasets presented in literature. Obtained results have been compared with other analytical and DL-based studies in literature which proves the accuracy for SOH prediction of series-connected LIB systems, clearly.

The key contributions of this paper can be highlighted as follows.

1. Capacity/voltage characteristics of series-connected LIB packs are generated by using existing popular datasets.
2. CWT is applied for feature specification scalograms for LIB SOH prediction.
3. The proposed classification technique can operate efficiently regardless of having small or large amount of data.
4. The easy applicability of the system is shown by solely using LIB voltage data for classification without needing any other measurement such as ampere-hour or calculating real-time capacity.
5. Proposed method can identify the battery SOH distribution in a LIB pack without needing to measure or test the batteries, separately.

3. Data configuration

In order to implement the proposed method for different types of LIB systems, the datasets presented in literature are used. Generally, real-time measured datasets contain charge and discharge characteristics of voltage (V), current (A), battery capacity (Ah) and temperature (C). In this study, it is focused on charge voltage characteristics with respect to battery capacity which slightly changes depending on SOH and degradation of the battery that has a relation to usage cycles. The reason for using the charge voltage characteristic is that it can be easily obtained even in simple systems while DL based prediction may be challenging as the number of batteries increase in a pack. In literature, datasets containing long-time charge and discharge characteristics are not numerous. In order to apply proposed methodology for degradation prediction, suitable datasets are chosen which are explained as follows.

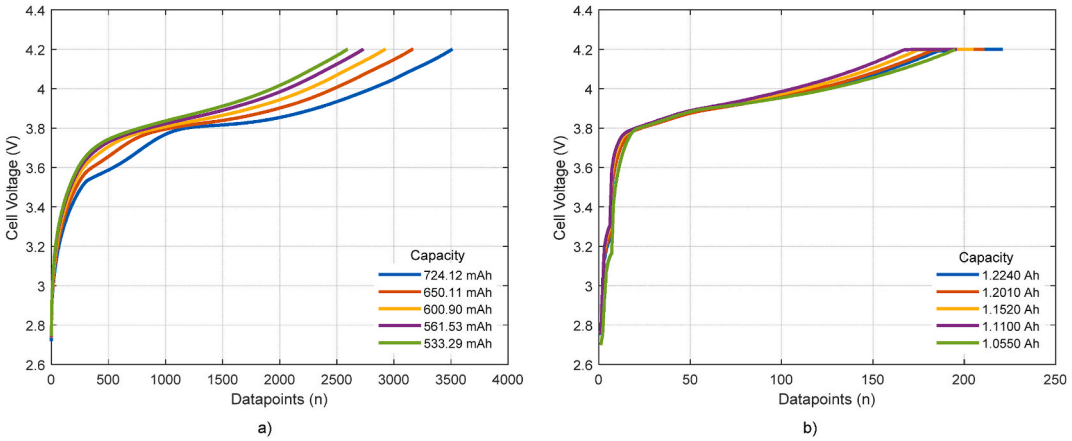

Fig. 1. Exemplary voltage characteristics for datasets; a) dataset-1, b) dataset-2.

Table 1
Series-connected battery pack classes.

Class	Series-Connected Battery Pack		
	4-cells	8-cells	8-cells
CL01	G-G-G-G	G-G-G-G-G-G-G-G	G-G-G-G-G-G-G-G
CL02	G-G-M-M	G-G-M-M-M-M-M-M	G-G-G-G-G-G-M-M
CL03	G-G-B-B	G-G-G-G-G-G-B-B	G-G-G-G-G-G-B-B
CL04	M-M-M-M	G-G-G-G-M-M-B-B	G-G-G-G-M-M-M-M
CL05	M-M-B-B	G-G-M-M-B-B-B-B	G-G-G-G-M-M-B-B
CL06	B-B-B-B	B-B-B-B-B-B-B-B	G-G-G-G-B-B-B-B
CL07	–	–	G-G-M-M-M-M-M-M
CL08	–	–	G-G-M-M-M-M-B-B
CL09	–	–	G-G-M-M-B-B-B-B
CL10	–	–	G-G-B-B-B-B-B-B
CL11	–	–	M-M-M-M-B-B-B-B
CL12	–	–	B-B-B-B-B-B-B-B

G: Good, M: Moderate, B: Bad.

3.1. Datasets

3.1.1. Dataset-1

Dataset-1 is chosen as Oxford Battery Degradation Dataset 1 (OBDD1) that includes long term battery ageing tests of 8 Kokam SLPB533459H4 740 mAh lithium-ion pouch cells [60]. In this dataset, there are 8 separate cells which have nominal voltage of 4.2 V. The dataset includes voltage, current and capacity characteristics for charge and discharge operation that are obtained in every 100 cycles. There are total of 70 uninterrupted cycles measurement data presented for each cell which have between 2500 and 3500 datapoints, approximately.

3.1.2. Dataset-2

CX2 prismatic battery degradation and ageing dataset (CX2-16) of Calce Battery Research Group is chosen as Dataset-2. The cells included in this dataset have 1350 mAh nominal capacity [61]. This dataset consists of more than 2000 cycles of charge and discharge data that every phase of charge and discharge operations have approximately 250 datapoints.

Each dataset given above are modelled by using the data acquired from battery charge/discharge equipment. Due to usage of different equipments or settings, the data obtained from given datasets are not sampled equally. Thus, number of datapoints for samples in each dataset and also even for the same dataset are different. For this reason, the necessary infrastructure for the serial battery data has been created by re-dimensioning the measurement data with the append method for each dataset. Charging characteristics of example cells for each dataset are given in Fig. 1 with corresponding cell capacities which show the change in voltage characteristics due to degradation. As seen in figure, the maximum and minimum capacity of an example cell included in Dataset-1 are 724.12 and 533.29 mAh while these values are 1.2240 and 1.0550 Ah for an example cell given in Dataset-2. The maximum cell voltages are almost same while charging characteristics of these cells differ especially for Dataset-1, significantly.

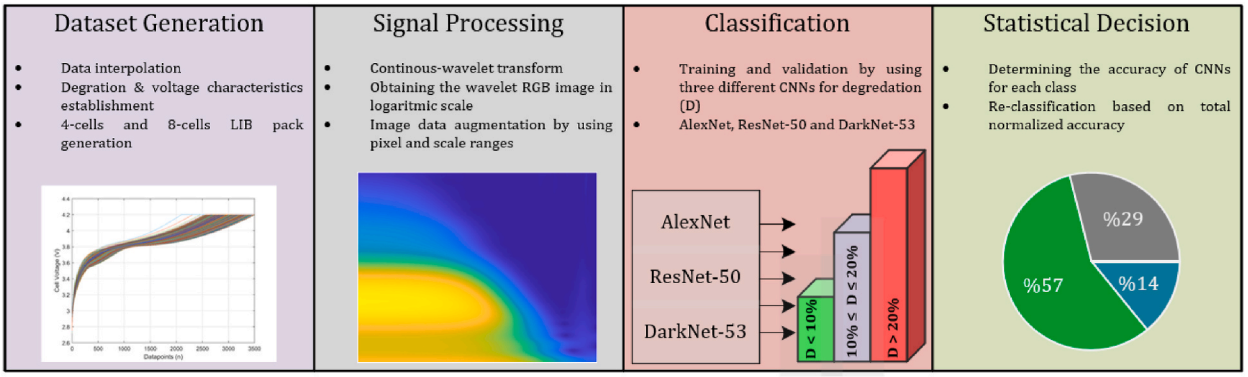

Fig. 2. The general block-diagram of proposed deep learning-based hybrid decision methodology.

3.2. Series-connected LIB dataset configuration

In this study, popular LIB related datasets are used for configuring a novel series-connected LIB pack voltage characteristics accordingly to corresponding LIB capacity. First, for this study the capacity data of cells are divided in three groups by 0%–10 % degraded, 10%–20 % degraded and more than 20 % degraded that are labelled as *Good*, *Moderate* and *Bad*, respectively. After that, by randomly combining the voltage values for corresponding capacity values, new data are generated for series-connected battery packs in two different types; 4-cells and 8-cells packs as given in Table 1. The maximum capacity of the cells for each cycle are used as an indicator to cluster the voltage data for generating new voltage characteristics data for 8 and 12 classes. For instance, in order to obtain a 4-cells *Good-Good-Bad-Bad* series-connected LIB pack, randomly chosen voltage data for 2 *Good* and 2 *Bad* samples are processed. By using this method, 200 random voltage-capacity characteristic samples for each class are obtained in order to apply processing and classification in next stages.

4. Methodology

In this study, a successful deep learning-based classification and decision method based on signal processing, deep learning algorithms and statistical performance indicators is used. In order to extract the features, classify and determine the most suitable class for input data of voltage and capacity of series-connected LIB packs; dataset generation, signal processing, classification and statistical decision stages are applied. As result, the performances of sole deep-learning and hybrid methods are achieved. In order to test the efficiency and accuracy of the proposed approach, voltage and capacity data of single and multi-LIBs are obtained. Also, data append and interpolation are applied to input data with the purpose of processing data with same number of dimensions in later stages. In the second stage, signal processing stage, the CWT is applied to the output data of the previous stage with the purpose of obtaining the scalograms for each voltage characteristic of LIB modules. The third stage of the proposed algorithm is feature extraction and classification by using deep learning-based algorithms. For this purpose, the AlexNet, ResNet-50, and Darknet-53 CNN architectures have been employed as feature extraction and classification techniques. The CNNs aforementioned above are trained and then tested by using various series-connected LIB pack characteristics. In the fourth stage of the proposed approach, the statistical decision stage, firstly statistical performance indicators are calculated by using the results of third stage. Subsequently, the classification results are obtained by using corresponding best values for each indicator. The general block-diagram of the proposed methodology is given in Fig. 2.

4.1. Continuous wavelet transform

Types of wavelet transform are almost the mostly employed signal-processing technique with the purpose of acquiring the time-and-frequency components of time-domain signals. In order to obtain the wavelet transform of a signal, the pre-determined wavelets namely mother wavelet and daughter wavelets are used. In order to examine the local features of a signal, this technique is commonly employed in the analysis of stable and non-stationary signals in a variety of domains. CWT is frequently chosen to analyse and obtain the features of time-varying signals by using different wavelets with different time and frequency scales. Therefore, the time-frequency resolution of CWT may help to obtain more detailed features compared to other signal processing methods such as Fourier or S-transform [62]. In order to obtain the features accurately, the main wavelet selection is crucial. In this study, Morse wavelets [63] are used in order to obtain scalogram images of signal data which method detailed in Section 5. The CWT transform, $F_{\omega}(a,b)$ of a given $f(t)$ function is expressed as,

$$F_{\omega}(a,b) = \frac{1}{|a|^{\frac{1}{2}}} \int_{-\infty}^{\infty} f(t)\overline{\psi}\left(\frac{t-b}{a}\right) dt \quad a,b \in R, a \neq 0 \tag{1}$$

Table 2
Parameters of AlexNet and ResNet – 50 architectures.

AlexNet Architecture Parameters			ResNet – 50 Architecture Parameters		
Operation	Filter Size/Stride	Output Size	Operation	Filter Size/Stride	Output Size
Convolution 1	$11 \times 11/4$	$55^2 \times 96$	Convolution 1	7×7, 64 Filters, Stride 2	112×112
Max. Pool 1	$3 \times 3/2$	$27^2 \times 96$	Convolution 2	3×3 Max Pool, Stride 2	56×56
Convolution 2	$5 \times 5/1$	$27^2 \times 256$	Convolution 2	$\begin{bmatrix} 1\times1, & 64 \\ 3\times3, & 64 \\ 1\times1, & 256 \end{bmatrix} \times 3$	
Max. Pool 2	$3 \times 3/2$	$13^2 \times 256$	Convolution 3	$\begin{bmatrix} 1\times1, & 128 \\ 3\times3, & 128 \\ 1\times1, & 256 \end{bmatrix} \times 4$	28×28
Convolution 3	$3 \times 3/1$	$13^2 \times 384$	Convolution 4	$\begin{bmatrix} 1\times1, & 256 \\ 3\times3, & 256 \\ 1\times1, & 1024 \end{bmatrix} \times 6$	14×14
Convolution 4	$3 \times 3/1$	$13^2 \times 384$	Convolution 5	$\begin{bmatrix} 1\times1, & 512 \\ 3\times3, & 512 \\ 1\times1, & 2048 \end{bmatrix} \times 3$	7×7
Convolution 5	$3 \times 3/1$	$13^2 \times 256$	Avg. Pool	–	1×1
Max. Pool 3	$3 \times 3/2$	$6^2 \times 256$	Fully Conn. Layer	–	1×1
Fully Conn. Layer 1	1×1	4096	SoftMax	–	1×1
Fully Conn. Layer 2	1×1	4096			
Fully Conn. Layer 3	1×1	1000			

Table 3
Parameters of DarkNet – 53 architecture.

DarkNet – 53 Architecture Parameters									
#	Operation	Input Size/Stride	Filter	Output	#	Operation	Input Size/Stride	Filter	Output
1	Convolution	3×3	32	256×256	13	Residual 3.1	–	–	32×32
2	Convolution	$3 \times 3/2$	64	128×128	14	Convolution	$3 \times 3/2$	512	16×16
3	Convolution 1.1	1×1	32	–	15	Convolution 4.1	1×1	256	–
4	Convolution 1.2	3×3	64	–	16	Convolution 4.2	3×3	512	
5	Residual 1.1	–	–	128×128	17	Residual 4.1	–	–	16×16
6	Convolution	$3 \times 3/2$	128	64×64	18	Convolution	$3 \times 3/2$	1024	8×8
7	Convolution 2.1	1×1	64	–	19	Convolution 5.1	1×1	512	–
8	Convolution 2.2	3×3	128	–	20	Convolution 5.2	3×3	1024	–
9	Residual 2.1			64×64	21	Residual 5.1		–	8×8
10	Convolution	$3 \times 3/2$	256	32×32	22	Avg. Pool	Global	–	–
11	Convolution 3.1	1×1	128	–	23	Connected	1000		–
12	Convolution 3.2	3×3	256	–	24	SoftMax	–	–	–

where a is scaling; b is translation factor and $\psi(t)$ is mother wavelet which is continuous in both time and frequency domain. The mother wavelet's primary role is to serve as a source function for the daughter wavelets, which are only scaled and translated variants of the mother wavelet [64].

4.2. Deep-learning methods

Recently, in literature there have been novel studies about neural networks proposed for data processing and classification. AlexNet, ResNet and DarkNet are popular and mostly used CNNs which are employed to solve image classification problems, optimally. Therefore, in this paper the CNNs aforementioned above are used to classify and detect battery degradation levels for multi-battery packs of LIBs, accurately.

4.2.1. AlexNet

AlexNet is one of the most preferred model and important milestone in visual recognition tasks of CNNs in image classification studies due to its novelty of the time of first proposed. This model contains eight layers which are combination of five convolutional layers and three fully linked layers [56]. The Rectified Linear Unit (ReLU) non-linearity and overlapping pooling which are the most important distinguishing features of the architecture that enables AlexNet to be a unique CNN which is also very fast compared to other popular CNNs for training process. In place of the tanh function, which was the industry standard at the time, AlexNet employs ReLU which has an edge over tanh in terms of training speed.

4.2.2. ResNet-50

In this study, one of the ResNet architectures, ResNet-50 model is used. ResNet models including different layer numbers and architectures are proposed in 2015 [57]. The novelty and performance of the ResNet model lies on its ability to overcome some

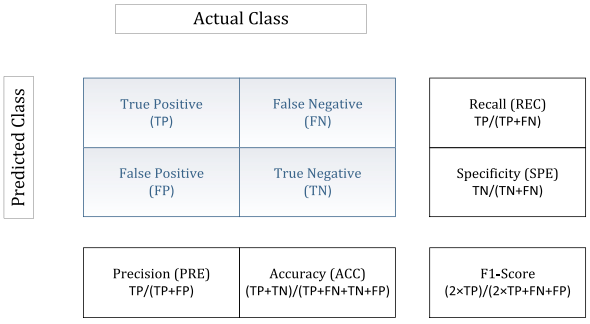

Fig. 3. Evaluation metrics calculations depending on actual and predicted classes.

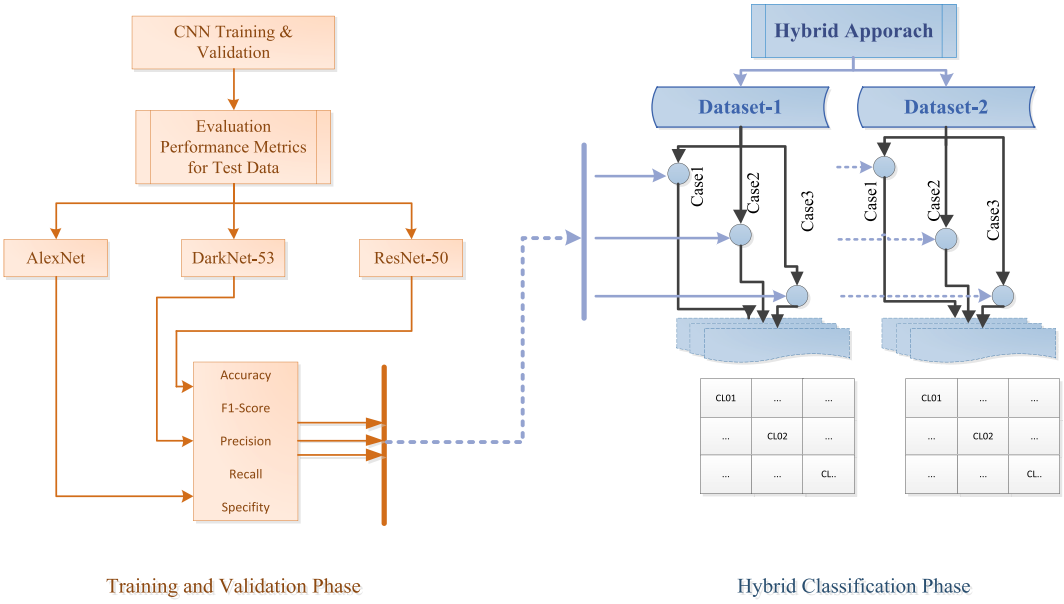

Fig. 4. The flowchart of proposed DL-based hybrid decision approach.

convergence problems. One of the most common problems in CNNs, vanishing gradient problem, should be eliminated in order to overcome the lowering training error rate down to zero. ResNet architectures also employ ReLu operations and skip-connection operators which greatly help to cope with this significant problem. The operational parameters of AlexNet and ResNet-50 are given in Table 2.

4.2.3. *DarkNet-53*

DarkNet-53 (namely YOLO-v3) is also a popular CNN which is proposed in 2018 by Redmon and Farhadi [58]. The DarkNet-53 an improved version of DarkNet-19 by employing more convolutional layers and ReLu operations. Unlike some other CNNS, in DarkNet-53 model input image is divided into an m × m grid just like a filter. All the parts of grids contain a bounding box and the network predicts *x*, *y*, *w* and *h* coordinate parameters of the bounding box in question. Thus, DarkNet-53 can predict the score called "objectness score" for each bounding box by using logistic regression. The obtained objectness score is used to determine whether there is an object in the area or not. The parameters of DarkNet-53 are given in Table 3.

4.3. *Performance evaluation metrics*

In literature, the evaluation metrics are generally employed to analyse the overall and subject-wise performances of classification by using computer-aided learning methods. In this study, the statistical performance indicators; F1-Score, Accuracy, Recall, Precision and Specificity are used to determine the values of best classification success for each class according to particular deep learning methods. The indicators aforementioned above are obtained by four sub-indicators namely, True Positive (TP), True Negative (TN), False Positive (FP), and False Negative (FN). The evaluation metrics are calculated by using the formulas given in Fig. 3 depending on actual and predicted classes.

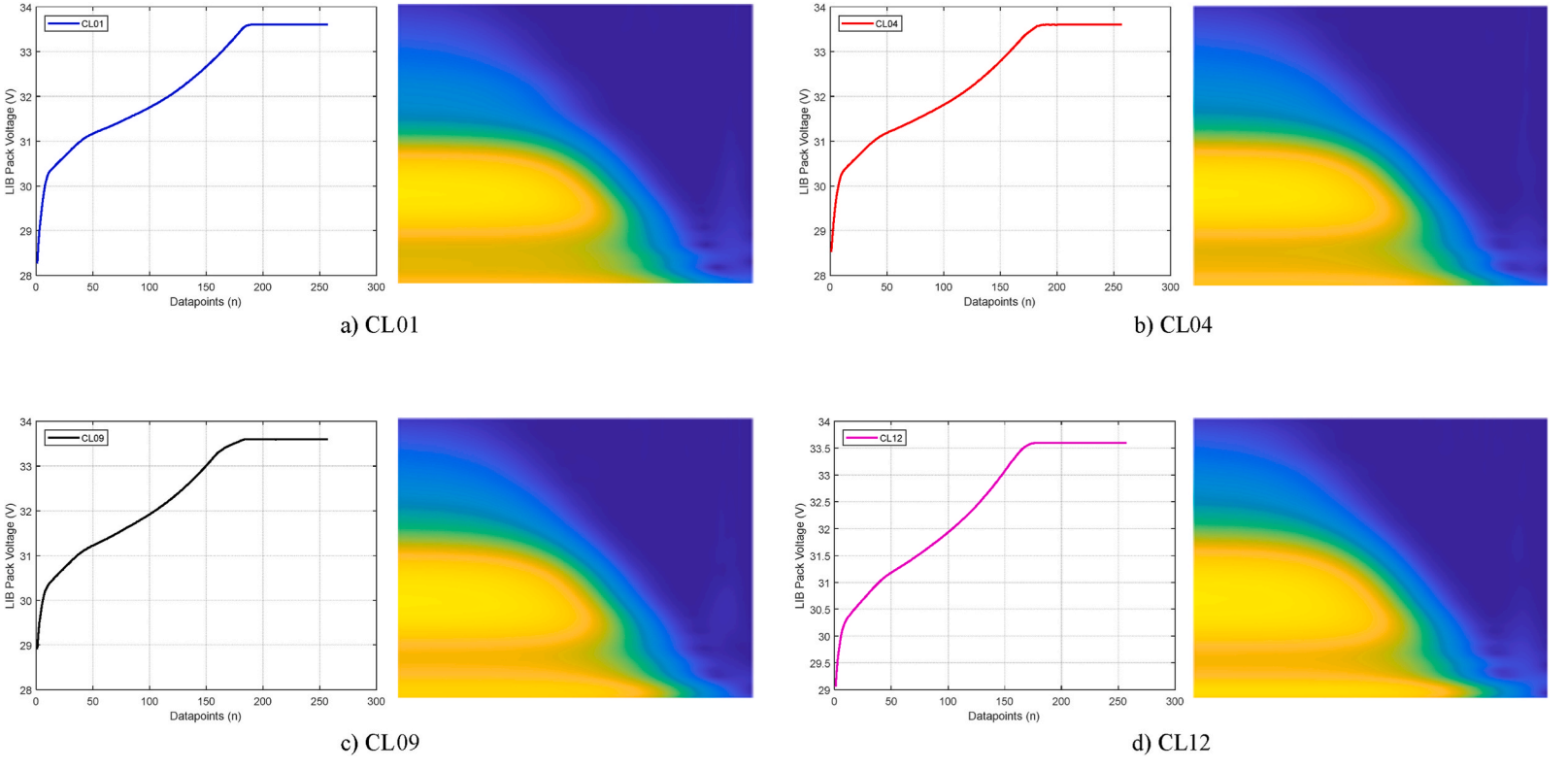

Fig. 5. Randomly generated voltage characteristics and scalograms of dataset-2 for 8-cells and 12-classes; a) CL01, b) CL04, c) CL09, d) CL12.

Table 4
Training parameters of deep learning algorithms.

Parameter	Value
Training algorithm	Stochastic gradient descent with momentum
Mini batch size	32
Maximum epoch	100
Initial learning rate	1×10^{-3}
Shuffle	Every-epoch

In order to implement and use the evaluation metrics for hybrid classification; first, the classification performances of CNNs are obtained. In the next step, the performance metrics are calculated for each class. With aim to provide the evaluation metrics in hybrid with CNNs, an algorithm is designed to use outputs of CNNs and/or evaluation metrics of validation data. The algorithm is basically, a decision method to classify an input depending on the highest value of metrics. The flowchart of statistical decision method is given in Fig. 4. In this proposed methodology, the class-wise metrics are used to determine the best result separately for the metrics aforementioned above.

4.4. Error indicators

In such classification problems, along with the accuracy metric there are some performance indicators that express the error rate of the proposed system. In this study, mean squared error (MSE), root mean square error (RMSE) and mean-absolute percentage error (MAPE) are used to show the efficacy of the proposed methodology The general equations of MSE, RMSE [37], MAE and MAPE [39] are given by (2) - (4) where n is the dimension size; $\hat{x}$ represents the predicted class whereas x represents the true class,

$$MSE = \frac{1}{n}\sum_{i=1}^{n}(\hat{x}_i - x_i)^2 \tag{2}$$

$$RMSE = \sqrt{\frac{1}{n}\sum_{i=1}^{n}(\hat{x}_i - x_i)^2} \tag{3}$$

$$MAE = \frac{1}{n}\sum_{i=1}^{n}|\hat{x}_i - x_i| \tag{4}$$

$$MAPE = \frac{1}{n}\sum_{i=1}^{n}\left|\frac{\hat{x}_i - x_i}{x_i}\right| \tag{5}$$

5. Results and discussion

Results and performances of the proposed hybrid methodology are presented in this section. As given in Section 3, series-connected LIB pack data generated by dataset-1 and dataset-2 used to train classification performances of AlexNet, ResNet-50 and DarkNet-53, separately. For each dataset, 2 types of LIB packs are taken into consideration as given in Table 1. Also, the evaluation metrics are calculated by using the validation data, then the proposed hybrid methodology is applied to test data for obtaining the performances of both CNNs and hybrid approach. Some example scalograms of wavelet transformation for voltage characteristics are given in Fig. 5 below. If figure is investigated, it can be seen that subtle differences in the voltage characteristics may express different results on the CWT transformed scalograms.

Also, it should be noted that the simulations and calculations of this study are performed on MATLAB® software running on Windows® computer with i7-3770K processor and 16 GB memory along with RTX2060 graphics card.

5.1. DL – based classification

In this section, there are total 3 cases are studied. In Case1, 6 classes of 4-cells LIB pack voltage-capacity characteristics are used for both datasets while 6 classes of 8-cells LIB pack characteristics are used in Case2. Also, for the Case3, 12 classes of 8-cells LIB pack characteristics are used for both datasets for validating the performance of the proposed method. Firstly, the CNNs are trained by using 140 training data and 60 validation data for each class and classification results are obtained; following that, the evaluation metrics are employed to obtain a better result for LIB pack degradation detection and classification. The training parameters for DL-based algorithms are chosen as given Table 4 below. The training algorithm for updating network parameters is chosen as stochastic gradient descent with momentum due to its characteristic of adding momentum term for reducing the oscillation of network parameters. Also, mini batch size and maximum epoch are chosen as given below after for better training performance while initial learning rate is chosen as 1×10^{-3} in order to achieve to best training and validation performance together without over-training.

For calculating the class-wise metrics, only the classification results of corresponding classes are used, for example the class-wise

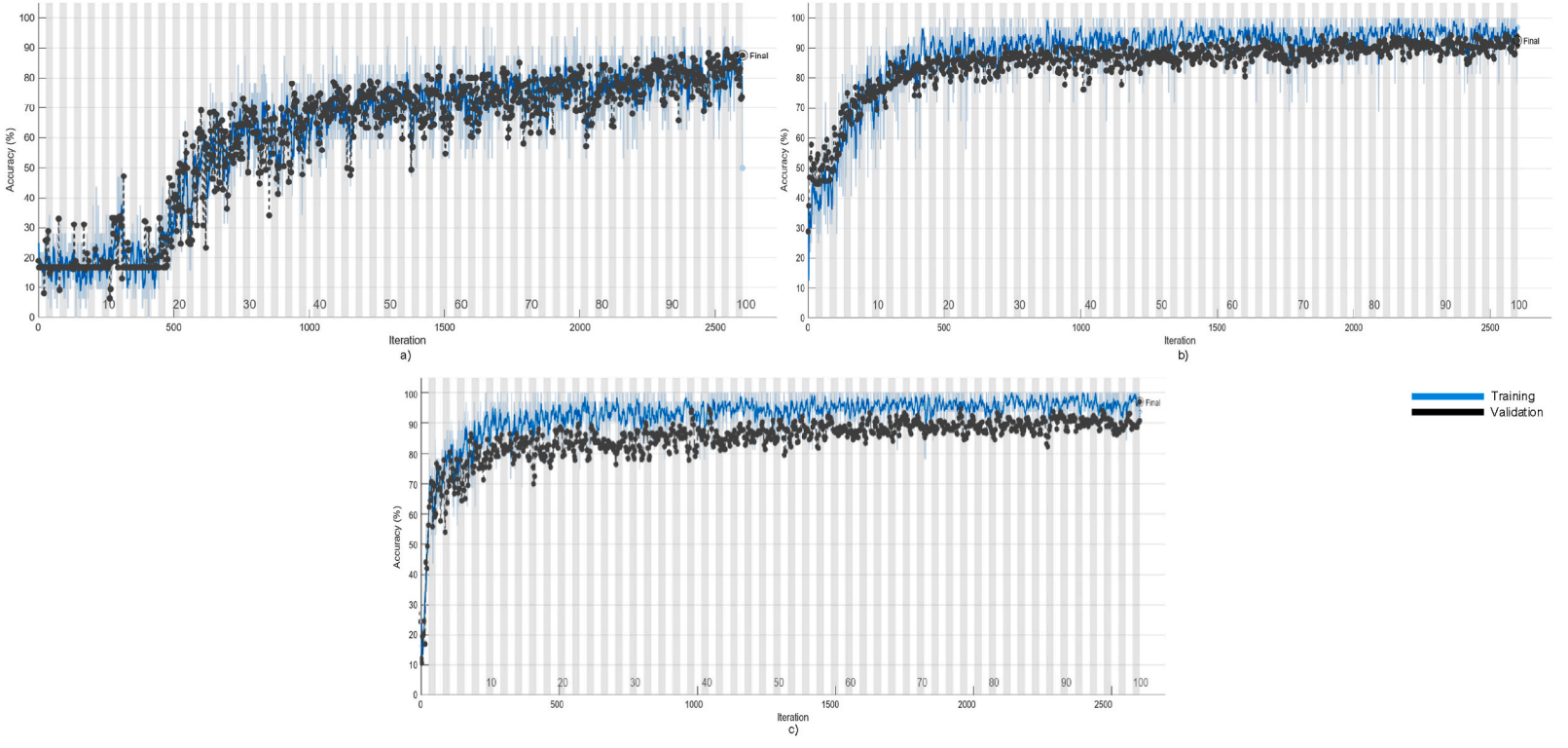

Fig. 6. Training and validation performances of algorithms on dataset-1 for 4-cells and 6-classes series LIB pack case; a) AlexNet, b) DarkNet-53, c) ResNet-50.

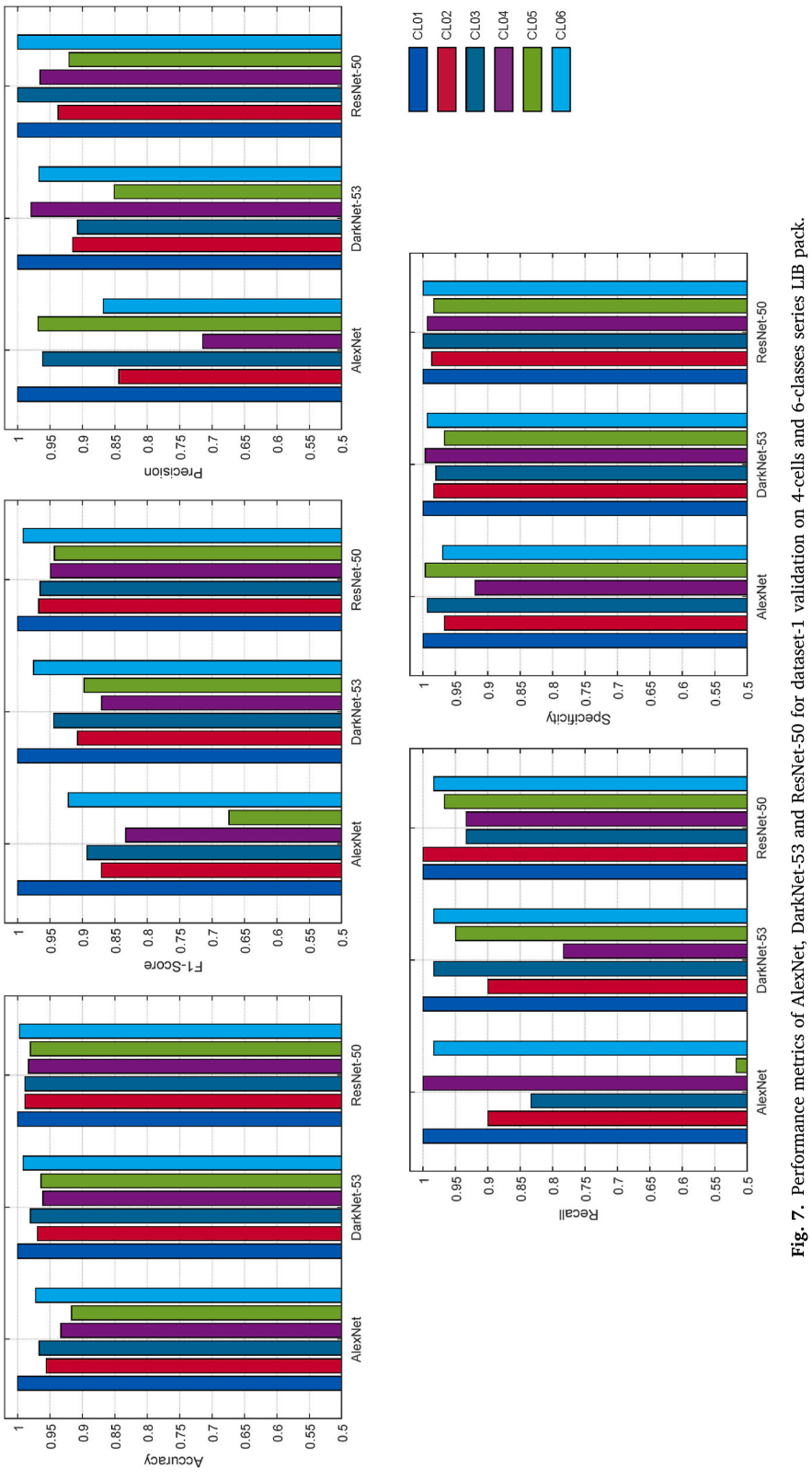

Fig. 7. Performance metrics of AlexNet, DarkNet-53 and ResNet-50 for dataset-1 validation on 4-cells and 6-classes series LIB pack.

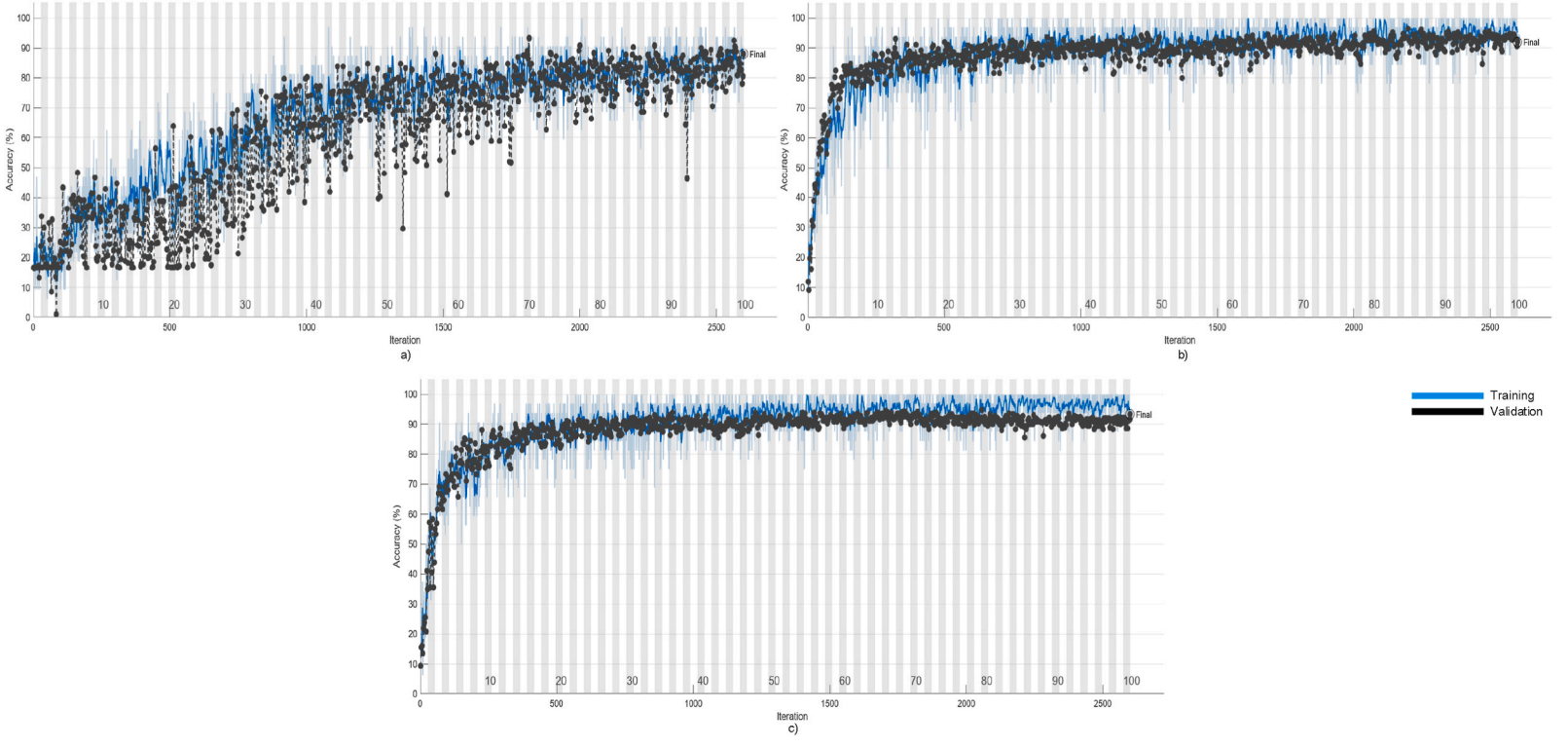

Fig. 8. Training and validation performances of algorithms on dataset-2 for 4-cells and 6-classes series LIB pack case; a) AlexNet, b) DarkNet-53, c) ResNet-50.

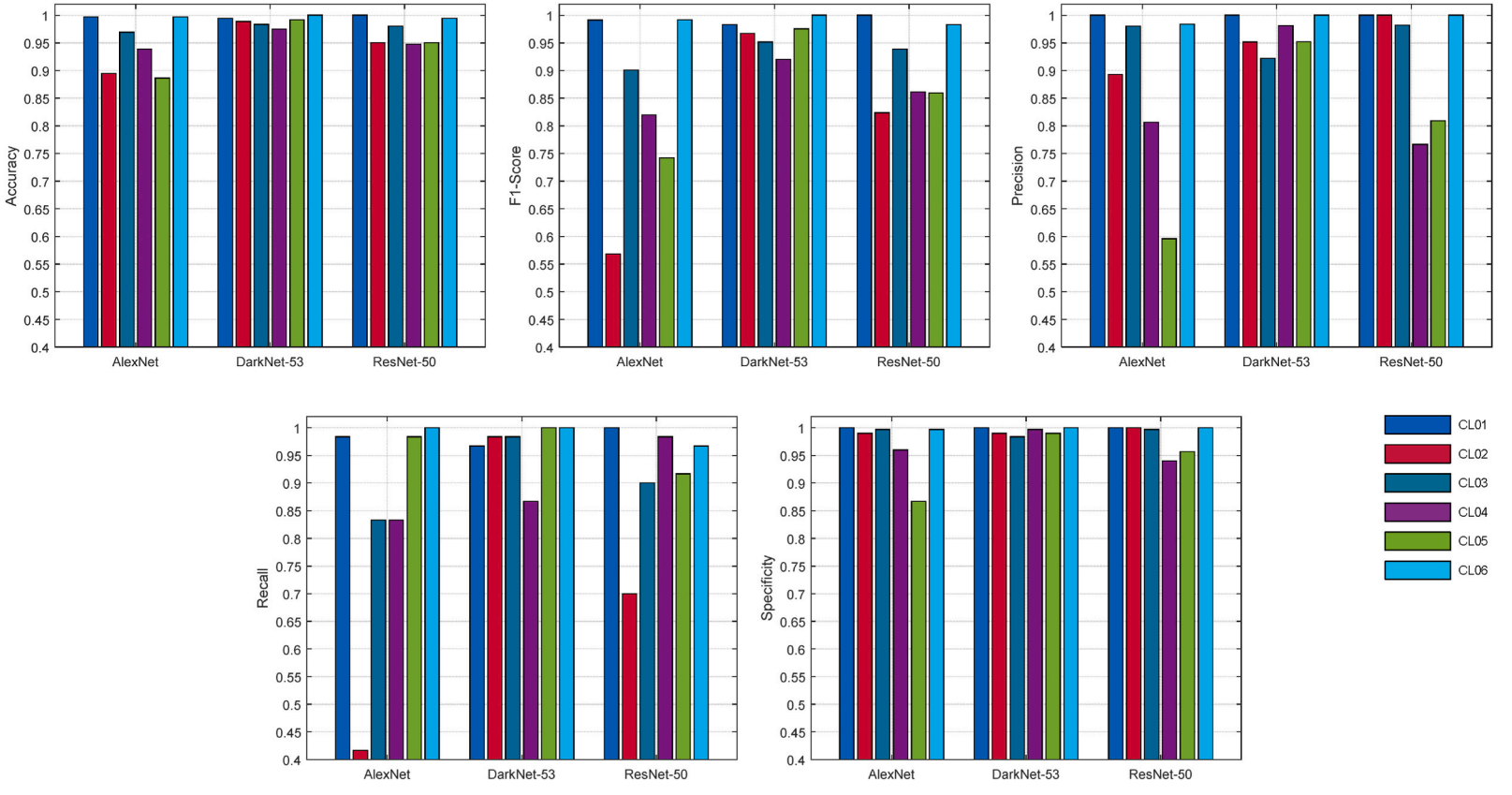

Fig. 9. Performance metrics of AlexNet, DarkNet-53 and ResNet-50 for dataset-2 validation on 4-cells and 6-classes series LIB pack.

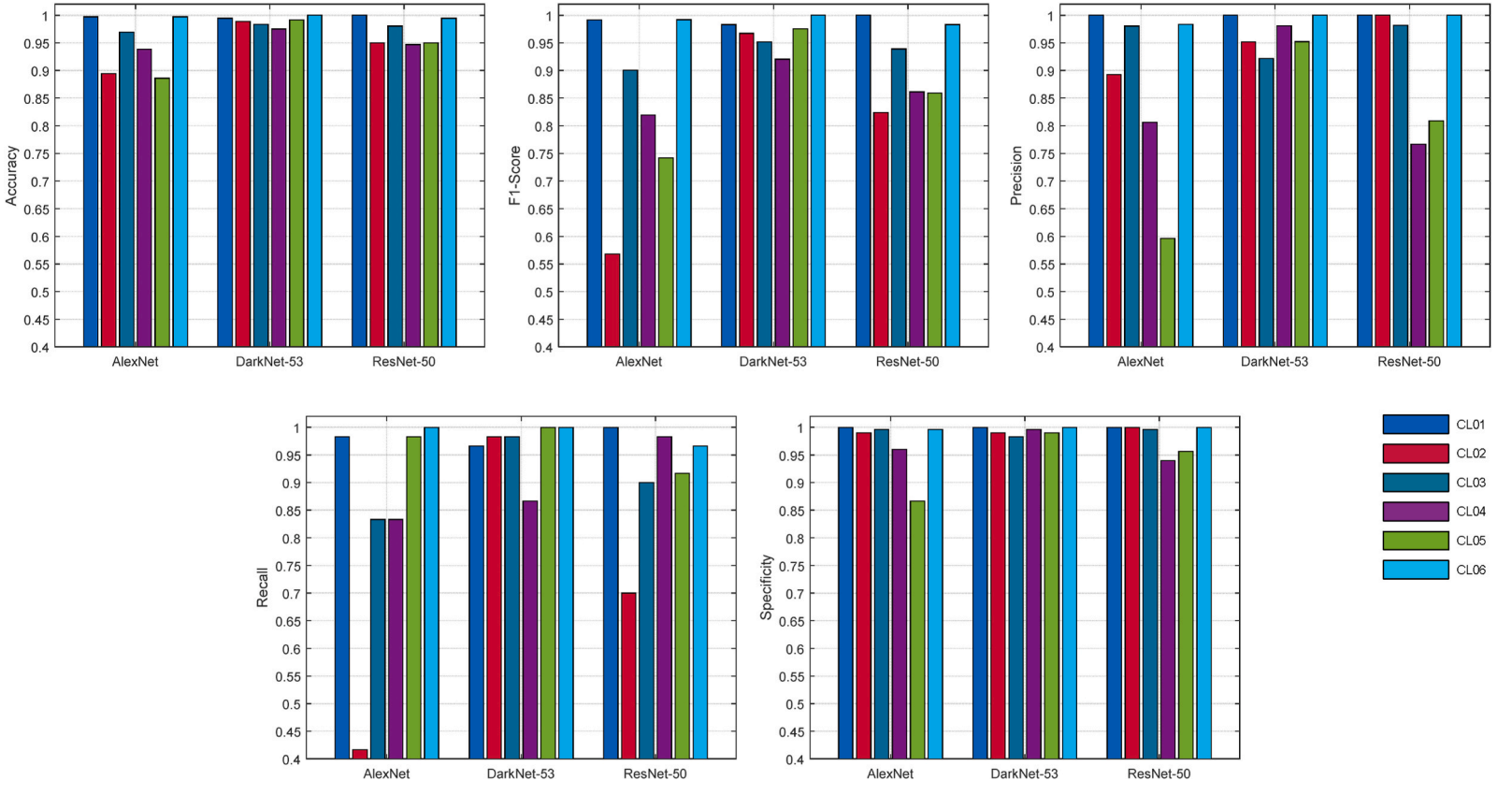

Fig. 10. Performance metrics of AlexNet, DarkNet-53 and ResNet-50 for dataset-1 validation on 8-cells and 6-classes series LIB pack.

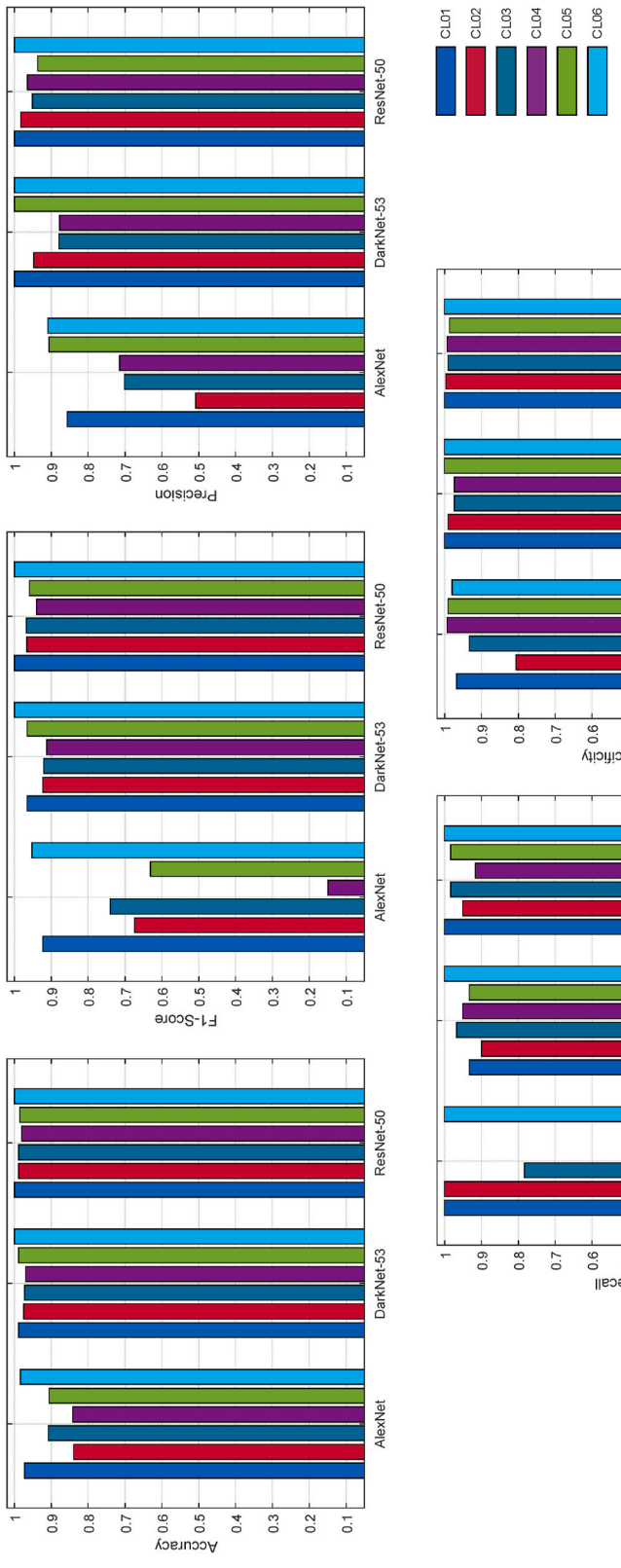

Fig. 11. Performance metrics of AlexNet, DarkNet-53 and ResNet-50 for dataset-2 validation on 8-cells and 6-classes series LIB pack.

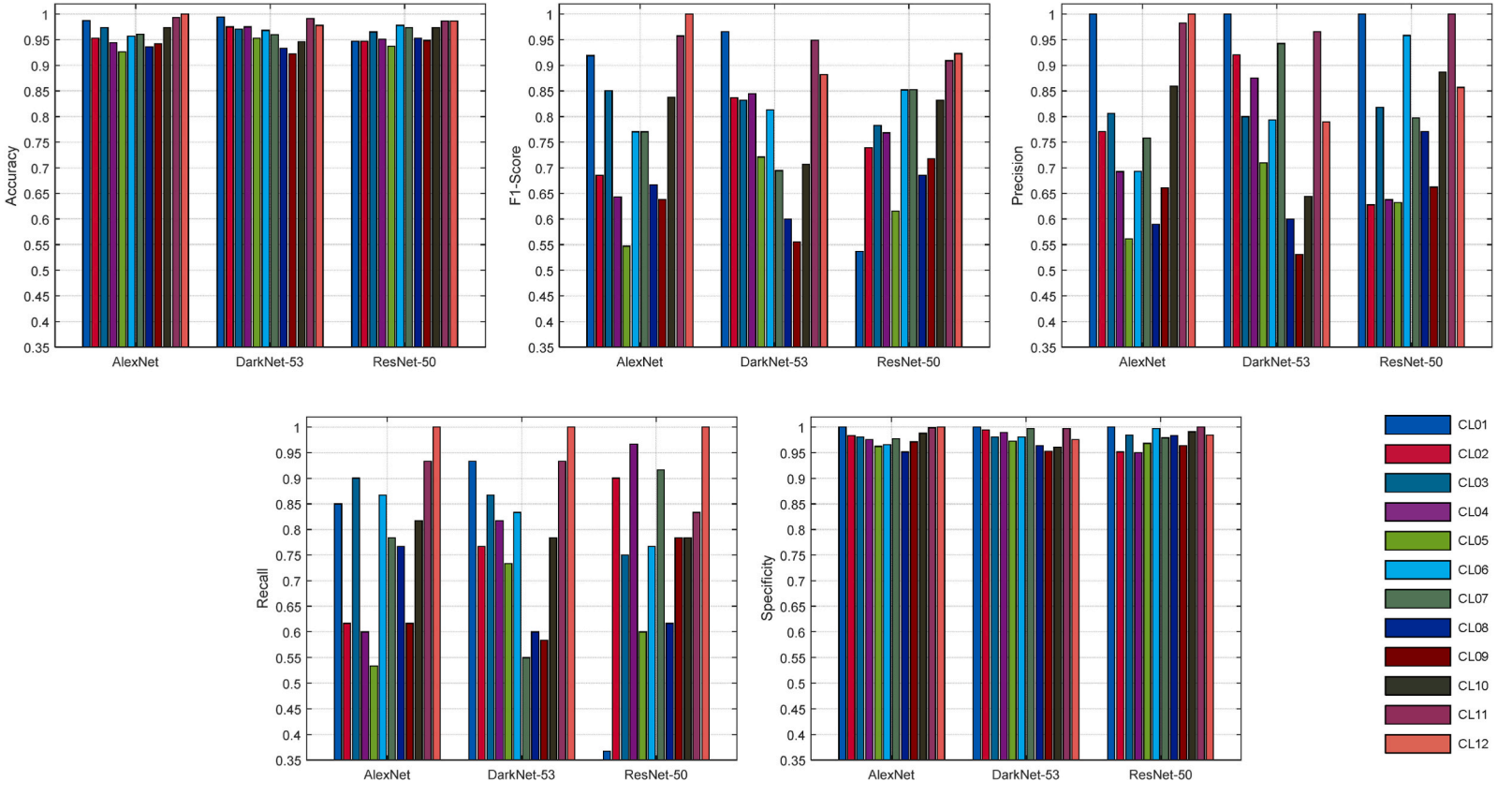

Fig. 12. Performance metrics of AlexNet, DarkNet-53 and ResNet-50 for dataset-1 validation on 8-cells and 12-classes series LIB pack.

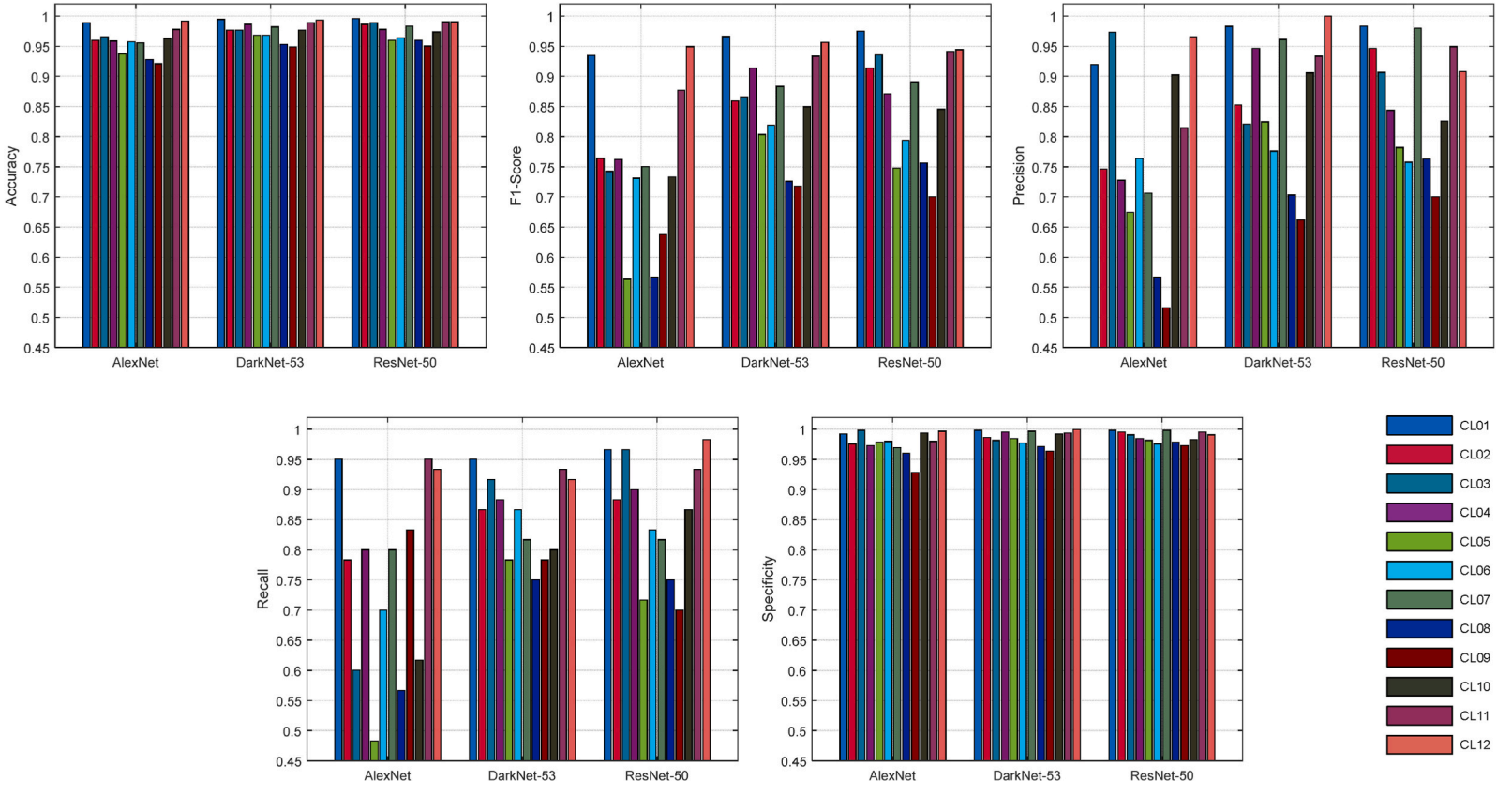

Fig. 13. Performance metrics of AlexNet, DarkNet-53 and ResNet-50 for dataset-2 validation on 8-cells and 12-classes series LIB pack.

Table 5
Single and hybrid classification performance of dataset-1.

Method		Overall Accuracy (%)		
		Case1	Case2	Case3
Single	AlexNet	85.67	86.83	76.58
	DarkNet-53	91.83	97.83	79.42
	ResNet-50	**94.50**	93.17	77.17
Hybrid	Accuracy	94.33	98.17	82.50
	F1-Score	94.33	98.17	79.92
	Precision	94.33	97.67	85.08
	Recall	89.67	**98.33**	78.17
	Specificity	94.33	97.67	**85.17**

accuracy is obtained by using (6) where TP_i is the true positive value of ith class.

$$ACC_i = \frac{TP_i}{number\ of\ validation\ data} \tag{6}$$

5.1.1. Case1 4-cells 6-classes series-connected LIB pack

5.1.1.1. Dataset-1. In the first analysis, the validation performances of AlexNet, ResNet-50 and DarkNet-53 are obtained as 87.22 %, 93.33 % and 96.94 % for AlexNet, DarkNet-53 and ResNet-50, respectively. The training and validation performance of simulation studies are given in Fig. 6. It has been observed that the validation performance of each algorithm is close to the training performance of that algorithm. Therefore, it can be stated that the training simulation is completed successfully without encountering problems such as over-training or under-training. In addition, the class-wise performance metrics of proposed DL-based algorithms are given in Fig. 7. It is observed that the most successfully predicted class is CL01 for all algorithms. On contrary, the algorithms have significantly low performance on CL04 and CL05 especially for F1-score, precision and recall.

5.1.1.2. Dataset-2. The training and validation performance of simulation studies are given in Fig. 8. It has been observed that the overall accuracy for validation data is obtained as 88.05 %, 91.94 % and 93.33 % for AlexNet, DarkNet-53 and ResNet-50, respectively. Therefore, it can be said that for both cases on dataset-1 and dataset-2, ResNet-50 have upper hand in overall performance. Also, the class-wise performance metrics of proposed algorithms are given in Fig. 9. It is observed that the most successfully predicted class is CL01 for all algorithms while, the performance metrics for CL05 and CL06 have decreased significantly compared to dataset-1.

5.1.2. Case2 8-cells 6-classes series-connected LIB pack

5.1.2.1. Dataset-1. The accuracy performances of validation data are obtained as 84.16 %, 96.66 % and 91.11 % for AlexNet, DarkNet-53 and ResNet-50. The DarkNet-53 has the best validation performance whereas AlexNet has lowest overall accuracy of which is lower more than 10 %. Also, the performance metrics are presented in Fig. 10. Recall and F1-score performances of AlexNet for CL02 is significantly low compared to other algorithms while CL01 and CL06 have very high performance for all algorithms.

5.1.2.2. Dataset-2. In this case, accuracy values for validation data are 72.50 %, 94.72 % and 97.22 % for AlexNet, DarkNet-53 and ResNet-50, respectively as class-wise metrics of validation performances of the algorithms are given in Fig. 11. The ResNet-50 algorithm has the best validation performance for all the classes while AlexNet has the worst performance for F1-score on CL04 that is 0.1493. Except CL04, AlexNet has lowest performance of 0.6304 for F1-score on CL05 and 0.5085 for precision on CL02.

5.1.3. Case3 8-cells 12-classes series-connected LIB pack

5.1.3.1. Dataset-1. Accuracy performance of classification by using DL-based methods obtained as 77.36 %, 78.33 % and 77.36 % for AlexNet, DarkNet-53 and ResNet-50 respectively. The class-wise metrics for 8-cells and 12-class series LIB pack of validation performances are given in Fig. 12. Except accuracy and specificity where the performances of algorithms are close to each other, DarkNet-53 and ResNet-50 have similar and better performance rather than AlexNet for the most classes. Overall, AlexNet has the most efficient performance on recall compared to other algorithms.

5.1.3.2. Dataset-2. The AlexNet, ResNet-50 and DarkNet-53 validation performances are obtained as 75.14 %, 85.56 % and 85.97 % that ResNet-50 algorithm has the best validation performance where DarkNet-53 has very close average accuracy. Also, class-wise metrics of validation performances are presented in Fig. 13. If figure is investigated, it can be seen that DarkNet-53 and ResNet-50 have better performances for most classes and metrics compared to AlexNet.

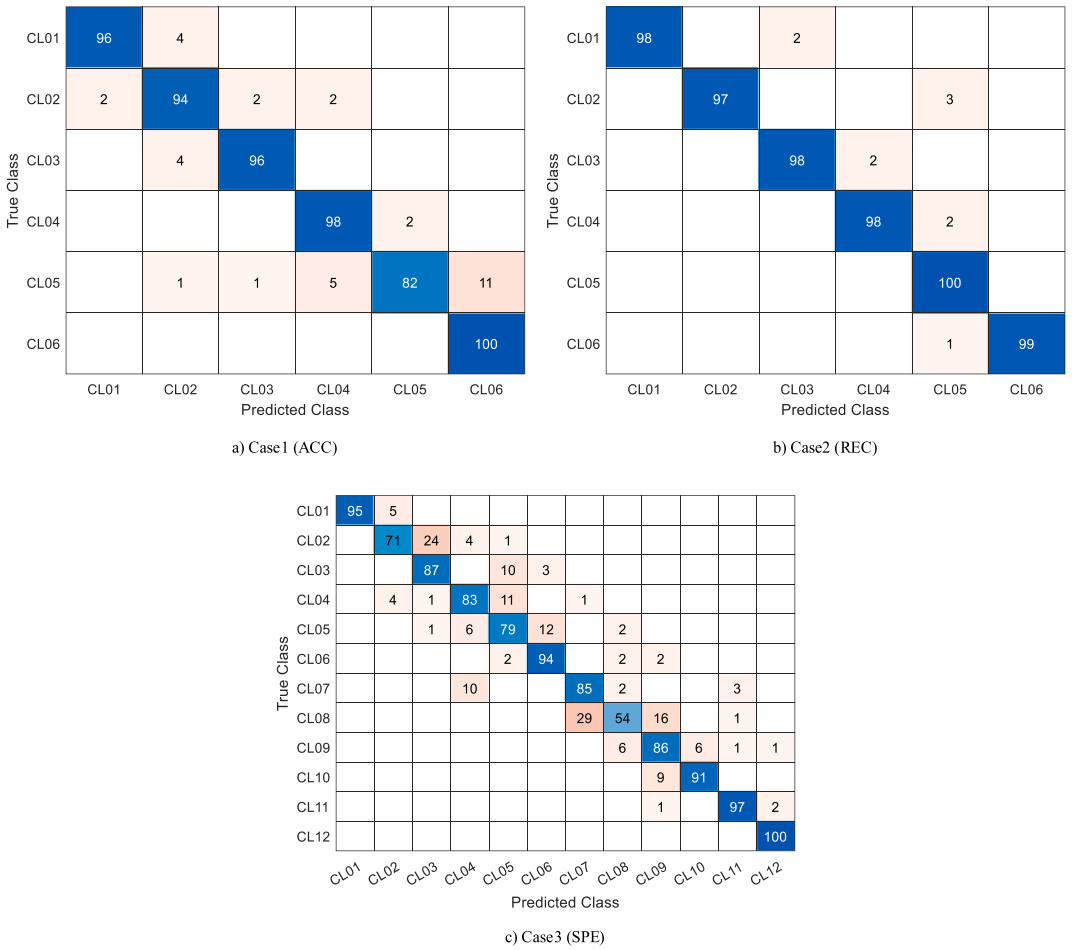

Fig. 14. Confusion matrices of hybrid-classification performance Dataset-1.

Table 6
Single and hybrid classification performance of dataset-2.

Method		Overall Accuracy (%)		
		Case1	Case2	Case3
Single	AlexNet	84.33	74.00	78.08
	DarkNet-53	92.50	97.00	83.25
	ResNet-50	94.67	97.50	84.83
Hybrid	Accuracy	**95.50**	**97.50**	85.33
	F1-Score	95.50	97.33	84.00
	Precision	93.33	97.50	**85.58**
	Recall	87.00	78.33	84.25
	Specificity	93.33	97.50	85.42

5.2. Hybrid classification

In this section, the CNNs and class-wise metrics are employed for classifying randomly generated LIB pack test data. For both datasets and 3 cases, 100 new data for each class are obtained and used according to flowchart given in Fig. 4 given in Section 4. The results show that using class-wise performance metrics may improve average classification performance.

5.2.1. Dataset-1

Hybrid and single-classification results for test data are presented in Table 5 for Case1, Case2 and Case3. In this table it can be seen that class-wise hybrid approach for Case2 and Case3 results with better classification performance. Especially, class-wise accuracy and F1-score values helps the algorithm to obtain better results compared to single-classification performance for Case2 while accuracy,

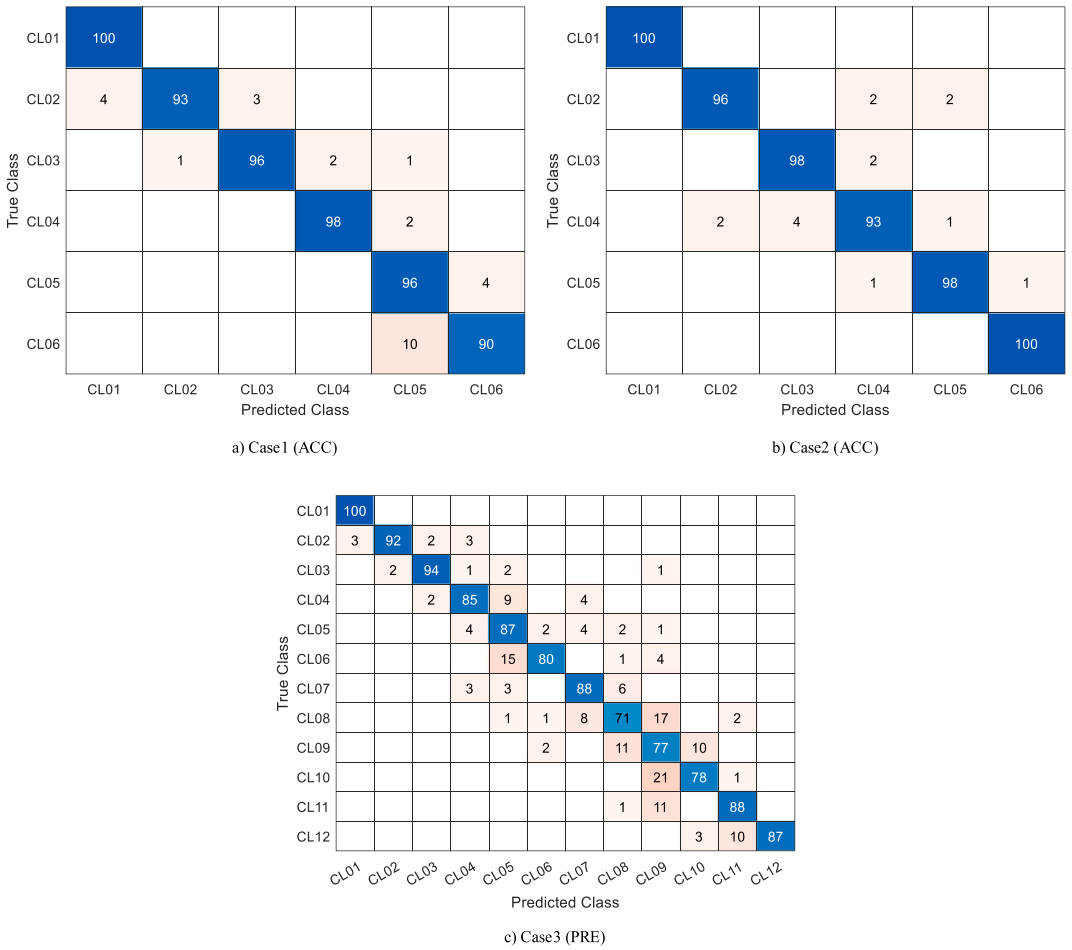

Fig. 15. Confusion matrices of hybrid-classification performance Dataset-2.

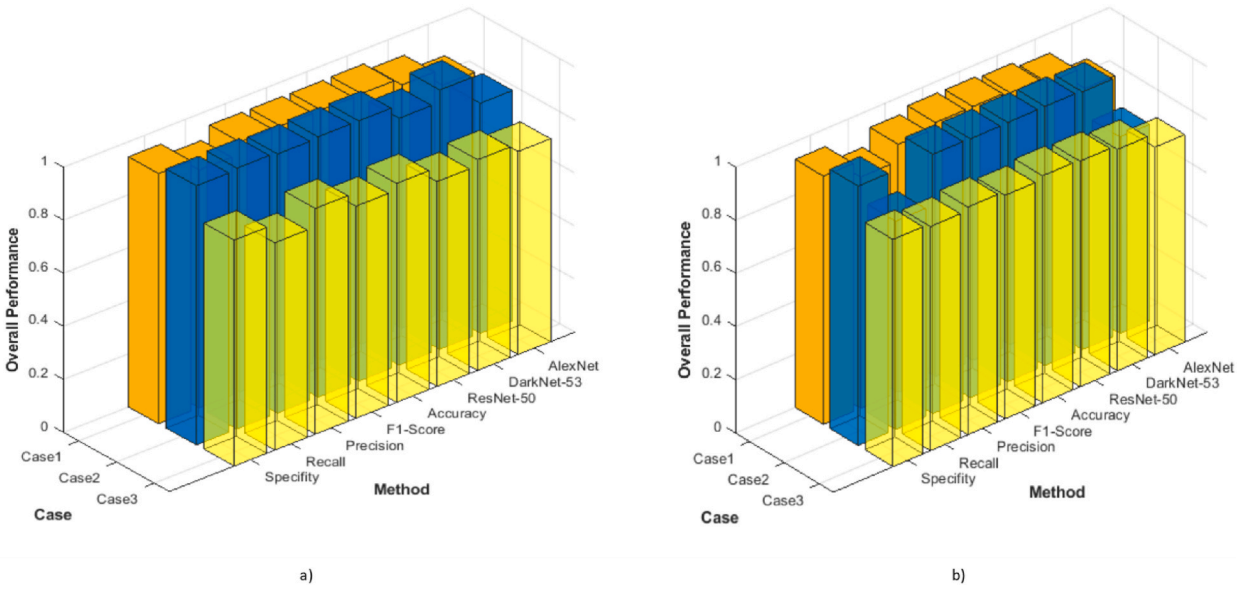

Fig. 16. Classification performance of proposed hybrid approach for; a) dataset-1, b) dataset-2.

Table 7
Performance comparison of single and hybrid approaches.

Case[a]	Best performance (%)			Worst performance (%)		
	Single	Hybrid	Improvement	Single	Hybrid	Improvement
D1C1	94.50	94.33	NA	85.67	89.67	4.4608
D1C2	97.83	98.33	0.5085	86.83	97.67	11.4057
D1C3	79.42	85.17	6.7512	76.58	78.17	2.0340
D2C1	94.67	95.50	0.8691	84.33	87.00	3.0689
D2C2	97.50	97.50	NA	74.00	78.33	5.5278
D2C3	78.08	85.58	8.7637	78.08	84.00	7.0476

[a] (D: Dataset, C: Case).

Table 8
Performance and error rate comparison with literature.

Study	Method	Dataset	Overall Accuracy	MSE	RMSE	MAE	MAPE	Average Classification Time per Sample (s)
Literature	BJ [22]	OBDD1	0.9761	–	0.1802	0.1434	–	33.1169
	ARMAX [22]	OBDD1	0.9673	–	0.2466	0.1931	–	15.3387
	ARX [22]	OBDD1	0.9635	–	0.2788	0.2252	–	1.6709
	OE [22]	OBDD1	0.9725	–	0.2075	0.1762	–	23.0048
	PDF [35]	NASA	–	–	0.9700	0.8200	–	–
	PDF [35]	CALCE	–	–	1.9400	1.5500	–	–
	Sequiental-8 DNN [36]	NASA	0.9400	–	–	–	–	–
	Linear-Regression [36]	NASA	0.8110	–	–	–	–	–
	R110-BLSTM [37]	DST	–	–	0.2520	0.3024	–	–
	HLM [39]	NASA	–	–	–	1.6730	2.8030	–
	CNN [39]	NASA	–	–	–	1.9430	3.1970	–
	LSTM [39]	NASA	–	–	–	2.1230	4.0130	–
	LSTM [40]	Experimental	–	–	0.0607	–	–	–
	LSTM [42]	NASA	–	–	0.2920	0.1980	–	–
	LSTM [42]	OBDD1	–	–	0.2160	0.1840	–	–
	BACO [43]	OBDD1	–	–	0.7700	0.6100	–	–
	SBEL [44]	OBDD1	–	–	0.7200	–	–	–
	LSTM-BP [45]	OBDD1	–	–	0.2200	–	–	–
	HIEPCC [46]	Experimental	–	–	0.5000	1.3000	–	–
	RNN [55]	NASA	–	–	1.4910	1.1730	–	0.1970
	LSTM [55]	NASA	–	–	0.9320	0.6720	–	0.4880
	CNN-LSTM [55]	NASA	–	–	0.8110	0.5380	–	0.4980
This Paper	Case1 (D1C1)	OBDD1	0.9433	0.0850	0.2915	0.0650	2.2194	0.0580
	Case2 (D1C2)	OBDD1	0.9833	0.0667	0.2582	0.0300	0.7056	0.0589
	Case3 (D1C3)	OBDD1	0.8517	0.3833	0.6191	0.2100	4.1875	0.0553
	Case1 (D2C1)	CX2-16	0.9550	0.0500	0.2236	0.0467	1.5778	0.0586
	Case2 (D2C2)	CX2-16	0.9750	0.0717	0.2677	0.0383	1.1083	0.0588
	Case3 (D2C3)	CX2-16	0.8558	0.3825	0.6185	0.2058	3.2630	0.0562

F1-score, precision and specificity outputs better results for Case3. On the other hand, since the accuracy of ResNet-50 is already high in Case1, the hybrid-classification may not be able to increase performance but since hybrid approach does not employ single-classification, the best hybrid result is obtained by 94.33 % by accuracy, F1-score and precision. For Case1 and Case2, class-wise accuracies are similar while for Case3, CL08 is the most notable class with lowest accuracy. Also, the confusion matrices for the best hybrid-performances are given in Fig. 14 namely accuracy, recall and specificity for Dataset-1 on Case1, Case2 and Case3.

5.2.2. Dataset-2

In this section, hybrid and single-classification approach are applied on Dataset-2 for all three cases and results presented in Table 6. By the results, it is concluded that that class-wise hybrid approach for all the cases results with better classification performance. Especially, class-wise accuracy increases the classification performance of Case1 and Case2 while precision helps the algorithm to converge to better results compared to single-classification performance for Case3. The hybrid approach converges to better results with 95.50 %, 97.50 % and 85.58 % or Case1, Case2 and Case3, respectively. For Case1 and Case3, CL02 and CL08 are have the lowest accuracy ratio respectively while CL04 is has the lowest ratio for Case2. Also, the confusion matrices for the best hybrid-performances are given in Fig. 15 namely accuracy and precision for Dataset-2 on Case1, Case2 and Case3.

5.3. Performance analysis and comparison

In this paper, classification and detection of SOH of the mostly used battery degradation datasets are achieved. The overall accuracy performance of proposed hybrid classification approach is given for both datasets in Fig. 16. In all cases except Case1 of Dataset-1,

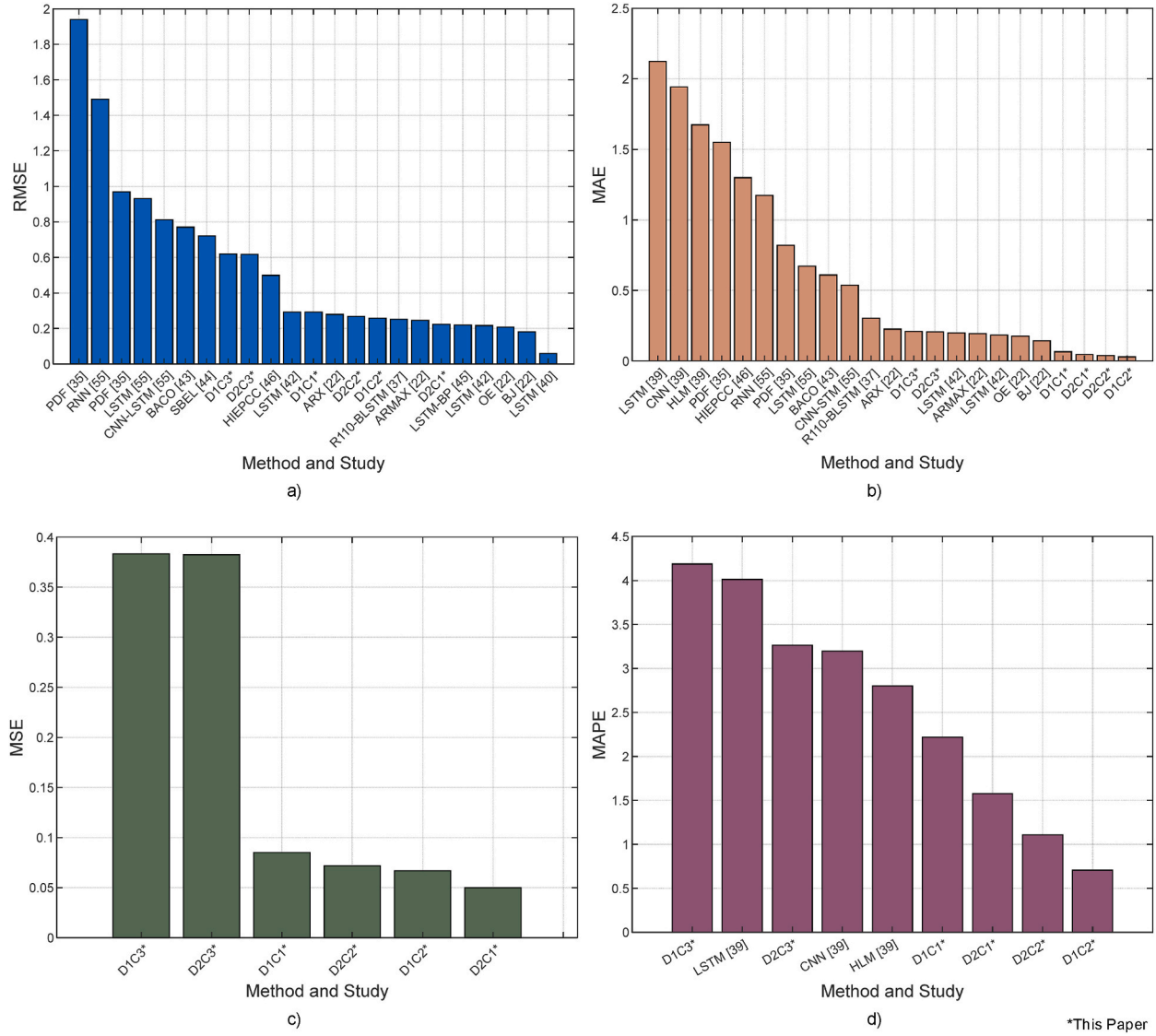

Fig. 17. Comparison chart of error metrics for proposed and literature studies.

hybrid approach results better performance than single-classification by using DL algorithms of AlexNet, DarkNet-53 and ResNet-50. Also, it is seen that if Tables 5 and 6 and Fig. 16 are investigated, using hybrid approaches based on any performance metric may result better that using a single DL method.

Also, the performance evaluations of overall accuracy and improvement rates for single and hybrid approaches employed in this paper are reported in Table 7. The hybrid-classification performance of Case1 on both datasets are either insignificantly lower and same with single-classification approach. The main reason for this lies in the distinct separation of classes in the first case study. On the other hand, as the characteristics of series-connected LIB classes gets close to each other as used in Case2 and Case3, hybrid-classification performance outpace the single-classification approach especially for the last case by 6.7512 and 8.7637. Also, the worst classification performances are presented in given table where hybrid approach obtains better results for all the cases. It can be concluded from the table that, as the complexity and intertwinement of the characteristics increase, the proposed hybrid approach can output better results, successfully.

In literature, most of the studies focus on SOH estimation of a single battery without taking series-connected LIB packs into consideration. Despite this, the accuracy rates and error rates of MSE, RMSE, MAE and MAPE of the studies presented in literature that are aimed at estimating the RUL for single or multiple batteries are compared and given in Table 8. It can be seen that the proposed hybrid-classification method achieves to good results compared to literature. For RMSE the proposed approach is better than most of the studies presented in literature, especially CNN, RNN and LSTM based deep learning approaches. Also, if MAE and MAPE values are investigated, some cases of proposed methodology for Case1 and Case2 on both datasets, achieve to lower error compared to other

Table 9
Overall comparison of error metrics for maximum, minimum and median values.

Metric	Maximum	Minimum	Median	Maximum of this study	Minimum of this study
MSE	0.3833	0.0500	0.0783	0.3833	0.0500
RMSE	1.9400	0.0607	0.2915	0.6191	0.2236
MAE	2.1230	0.0300	0.2252	0.2058	0.0300
MAPE	4.1875	0.7056	2.8030	4.1875	0.7056

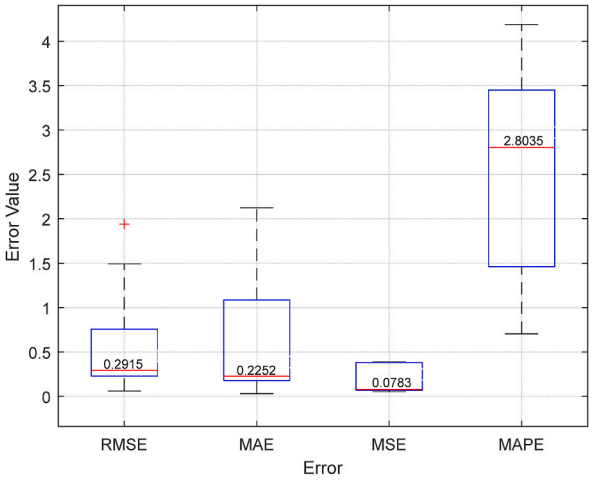

Fig. 18. Summary chart of error metrics for maximum, minimum and median values.

studies given in the comparison table. In addition, the average classification per sample is given that the highest consumed time is 0.0589 s which is acceptable for even online integrated decision systems with high number of clients.

In addition, the RMSE, MAE, MSE and MAPE comparison charts of the proposed approach and other studies are given by Fig. 17. It can be concluded that lower number of LIBs in a battery pack results better classification for predetermined classes given in Section 3. Despite this, the proposed method's error values are mostly lower than most of the studies presented in literature for both datasets and different cases.

In addition, the maximum, minimum and median values of error metrics along with comparison with the results of this study are reported in Table 9. It can be seen from the table that, especially for RMSE, MAE and MAPE, the performance of the proposed approach can be verified with lower metric values compared to median values as, 0.2236, 0.0300 and 0.7056, respectively. In addition, the chart for the comparison of error metrics is presented in Fig. 18. It is seen in figure that the median values of each error metric for its own class are indicated with red lines as 0.2915, 0.2252, 0.0783 and 2.8030 for RMSE, MAE, MSE and MAPE, respectively.

In addition, it can be said that in literature, a few studies focus on environmental conditions such as temperature of LIBs for charging and discharging operations. In this study, the first dataset (OBBD1) has presented the temperature data which is between 39.62 and 41.24 °C while the second dataset (CX2-16) does not include the temperature data for battery operations. In addition, in this paper, voltage characteristics data for different kinds of batteries presented in datasets are employed for indicating the efficiency of the proposed hybrid approach. Thus, it is thought that a successful classification and detection can be achieved without any problems regarding the change in type of battery and small temperature changes. However, different improvements and additions may be required for studies that focus on battery status where battery operating conditions change significantly.

6. Conclusion

In this paper, first, series-connected LIB pack voltage-capacity characteristics for SOH prediction are generated for mostly used LIB datasets namely Oxford Battery Degradation Dataset 1 and Calce CX2 prismatic battery degradation and ageing dataset. The 4 and 8-cells LIB packs characteristics are generated and processed by CWT and the feature scalograms are processed by three different CNNs, AlexNet, DarkNet-53 and ResNet-50 before obtaining the metrics for hybrid-classification stage. The results showed that the overall accuracy decreases as the number of classes in series-connected LIB increases but at the same time it can be said that the worst classification accuracy is 85.17 % which is better than most studies related to engineering. The results showed that the proposed method can achieve a highly accurate SOH estimation with hybrid-classification. The MSE, RMSE and MAPE values of the SOH prediction on the OBBD1 and CX2-16 datasets are between 0.0500 and 0.03833; 0.2236–0.6191 and 0.7056–4.1875, respectively. Also, the proposed method uses charging voltage signal features obtained by CWT which can provide complete representation of signal characteristics. In addition, by implementing a simple but efficient hybrid decision approach based on class-wise metrics, the

classification performance increases in significant manner particularly for classes with similar characteristics. The main contributions of this study as follows.

(1) The proposed series-connected LIB pack voltage characteristic along with CWT based feature-extraction approach can successfully generate as many as SOH scalograms by using limited amount of data.
(2) The AlexNet, DarkNet-53 and ResNet-50 based single-classification approaches are shown to achieve good results especially by using DarkNet-53 and ResNet-50 algorithms.
(3) The hybrid-classification approach can increase the accuracy by employing class-wise performance metrics in a duration not more than 59 ms per sample.
(4) Compared to the methods presented in similar studies in the literature, the proposed hybrid algorithm has better performance than most of the studies in terms of both accuracy and detection time.

Data availability

Data will be made available on request.

Declaration of competing interest

The authors declare that they have no known competing financial interests or personal relationships that could have appeared to influence the work reported in this paper.

References

[1] J. Wang, Y. Xiang, Fast modeling of the capacity degradation of lithium-ion batteries via a conditional temporal convolutional encoder–decoder, IEEE Transactions on Transportation Electrification 8 (2) (Jun. 2022) 1695–1709, https://doi.org/10.1109/TTE.2021.3128018.
[2] M. Dong, et al., State of health (SOH) assessment for LIBs based on characteristic electrochemical impedance, J. Power Sources 603 (May 2024) 234386, https://doi.org/10.1016/j.jpowsour.2024.234386.
[3] Y. Jiang, J. Jiang, C. Zhang, W. Zhang, Y. Gao, N. Li, State of health estimation of second-life LiFePO4 batteries for energy storage applications, J. Clean. Prod. 205 (Dec. 2018) 754–762, https://doi.org/10.1016/j.jclepro.2018.09.149.
[4] B. Xia, Z. Qin, H. Fu, Rapid estimation of battery state of health using partial electrochemical impedance spectra and interpretable machine learning, J. Power Sources 603 (May 2024) 234413, https://doi.org/10.1016/j.jpowsour.2024.234413.
[5] Y. Shang, S. Wang, N. Tang, Y. Fu, K. Wang, Research progress in fault detection of battery systems: a review, J. Energy Storage 98 (Sep. 2024) 113079, https://doi.org/10.1016/j.est.2024.113079.
[6] C.R. Birkl, M.R. Roberts, E. McTurk, P.G. Bruce, D.A. Howey, Degradation diagnostics for lithium ion cells, J. Power Sources 341 (Feb. 2017) 373–386, https://doi.org/10.1016/j.jpowsour.2016.12.011.
[7] K.A. Severson, et al., Data-driven prediction of battery cycle life before capacity degradation, Nat. Energy 4 (5) (Mar. 2019) 383–391, https://doi.org/10.1038/s41560-019-0356-8.
[8] I. Jorge, T. Mesbahi, A. Samet, R. Boné, Time series feature extraction for lithium-ion batteries state-of-health prediction, J. Energy Storage 59 (Mar. 2023) 106436, https://doi.org/10.1016/j.est.2022.106436.
[9] L. Mai, M. Yan, Y. Zhao, Track batteries degrading in real time, Nature 546 (7659) (Jun. 2017) 469–470, https://doi.org/10.1038/546469a.
[10] F. Yang, Y. Xie, Y. Deng, C. Yuan, Predictive modeling of battery degradation and greenhouse gas emissions from U.S. state-level electric vehicle operation, Nat. Commun. 9 (1) (Jun. 2018) 2429, https://doi.org/10.1038/s41467-018-04826-0.
[11] J. Li, L. Wang, C. Lyu, H. Wang, X. Liu, New method for parameter estimation of an electrochemical-thermal coupling model for LiCoO2 battery, J. Power Sources 307 (Mar. 2016) 220–230, https://doi.org/10.1016/j.jpowsour.2015.12.058.
[12] Y. Song, D. Liu, C. Yang, Y. Peng, Data-driven hybrid remaining useful life estimation approach for spacecraft lithium-ion battery, Microelectron. Reliab. 75 (Aug. 2017) 142–153, https://doi.org/10.1016/j.microrel.2017.06.045.
[13] S. Hong, Z. Zhou, E. Zio, W. Wang, An adaptive method for health trend prediction of rotating bearings, Digit. Signal Process. 35 (Dec. 2014) 117–123, https://doi.org/10.1016/j.dsp.2014.08.006.
[14] Z. Chen, L. Chen, W. Shen, K. Xu, Remaining useful life prediction of lithium-ion battery via a sequence decomposition and deep learning integrated approach, IEEE Trans. Veh. Technol. 71 (2) (Feb. 2022) 1466–1479, https://doi.org/10.1109/TVT.2021.3134312.
[15] X. Xu, N. Chen, A state-space-based prognostics model for lithium-ion battery degradation, Reliab. Eng. Syst. Saf. 159 (Mar. 2017) 47–57, https://doi.org/10.1016/j.ress.2016.10.026.
[16] X. Hu, D. Cao, B. Egardt, Condition monitoring in advanced battery management systems: moving horizon estimation using a reduced electrochemical model, IEEE ASME Trans. Mechatron. 23 (1) (Feb. 2018) 167–178, https://doi.org/10.1109/TMECH.2017.2675920.
[17] W. He, N. Williard, M. Osterman, M. Pecht, Prognostics of lithium-ion batteries based on Dempster–Shafer theory and the Bayesian Monte Carlo method, J. Power Sources 196 (23) (Dec. 2011) 10314–10321, https://doi.org/10.1016/j.jpowsour.2011.08.040.
[18] M. V Micea, L. Ungurean, G.N. Cârstoiu, V. Groza, Online state-of-health assessment for battery management systems, IEEE Trans. Instrum. Meas. 60 (6) (Jun. 2011) 1997–2006, https://doi.org/10.1109/TIM.2011.2115630.
[19] N. Baba, H. Yoshida, M. Nagaoka, C. Okuda, S. Kawauchi, Numerical simulation of thermal behavior of lithium-ion secondary batteries using the enhanced single particle model, J. Power Sources 252 (Apr. 2014) 214–228, https://doi.org/10.1016/j.jpowsour.2013.11.111.
[20] S. Khaleghi Rahimian, S. Rayman, R.E. White, Extension of physics-based single particle model for higher charge–discharge rates, J. Power Sources 224 (Feb. 2013) 180–194, https://doi.org/10.1016/j.jpowsour.2012.09.084.
[21] Q. Miao, L. Xie, H. Cui, W. Liang, M. Pecht, Remaining useful life prediction of lithium-ion battery with unscented particle filter technique, Microelectron. Reliab. 53 (6) (Jun. 2013) 805–810, https://doi.org/10.1016/j.microrel.2012.12.004.
[22] G. Yüksek, A. Alkaya, A novel state of health estimation approach based on polynomial model for lithium-ion batteries, Int. J. Electrochem. Sci. 18 (5) (May 2023) 100111, https://doi.org/10.1016/j.ijoes.2023.100111.
[23] S. Cui, S. Lyu, Y. Ma, K. Wang, Improved informer PV power short-term prediction model based on weather typing and AHA-VMD-MPE, Energy 307 (Oct. 2024) 132766, https://doi.org/10.1016/j.energy.2024.132766.
[24] V. Safavi, N. Bazmohammadi, J.C. Vasquez, J.M. Guerrero, Battery state-of-health estimation: a step towards battery digital twins, Electronics (Basel) 13 (3) (Jan. 2024) 587, https://doi.org/10.3390/electronics13030587.
[25] L. Driscoll, S. de la Torre, J.A. Gomez-Ruiz, Feature-based lithium-ion battery state of health estimation with artificial neural networks, J. Energy Storage 50 (Jun. 2022) 104584, https://doi.org/10.1016/j.est.2022.104584.

[26] M.S. Hossain Lipu, et al., Deep learning enabled state of charge, state of health and remaining useful life estimation for smart battery management system: methods, implementations, issues and prospects, J. Energy Storage 55 (Nov. 2022) 105752, https://doi.org/10.1016/j.est.2022.105752.
[27] G. Ma, Y. Zhang, C. Cheng, B. Zhou, P. Hu, Y. Yuan, Remaining useful life prediction of lithium-ion batteries based on false nearest neighbors and a hybrid neural network, Appl. Energy 253 (Nov. 2019) 113626, https://doi.org/10.1016/j.apenergy.2019.113626.
[28] Z. Bao, J. Jiang, C. Zhu, M. Gao, A new hybrid neural network method for state-of-health estimation of lithium-ion battery, Energies 15 (12) (Jun. 2022) 4399, https://doi.org/10.3390/en15124399.
[29] P. Tagade, et al., Deep Gaussian process regression for lithium-ion battery health prognosis and degradation mode diagnosis, J. Power Sources 445 (Jan. 2020) 227281, https://doi.org/10.1016/j.jpowsour.2019.227281.
[30] M. Raman, V. Champa, V. Prema, State of health estimation of lithium ion batteries using recurrent neural network and its variants, in: 2021 IEEE International Conference on Electronics, Computing and Communication Technologies (CONECCT), IEEE, Jul. 2021, pp. 1–6, https://doi.org/10.1109/CONECCT52877.2021.9622557.
[31] J. Liu, et al., PEMFC residual life prediction using sparse autoencoder-based deep neural network, IEEE Transactions on Transportation Electrification 5 (4) (Dec. 2019) 1279–1293, https://doi.org/10.1109/TTE.2019.2946065.
[32] J. Zhang, P. Wang, Q. Gong, Z. Cheng, SOH estimation of lithium-ion batteries based on least squares support vector machine error compensation model, Journal of Power Electronics 21 (11) (Nov. 2021) 1712–1723, https://doi.org/10.1007/s43236-021-00307-8.
[33] M.-S. Park, J. Lee, B.-W. Kim, SOH estimation of Li-ion battery using discrete wavelet transform and long short-term memory neural network, Appl. Sci. 12 (8) (Apr. 2022) 3996, https://doi.org/10.3390/app12083996.
[34] K. Park, Y. Choi, W.J. Choi, H.-Y. Ryu, H. Kim, LSTM-Based battery remaining useful life prediction with multi-channel charging profiles, IEEE Access 8 (2020) 20786–20798, https://doi.org/10.1109/ACCESS.2020.2968939.
[35] Z. Lin, Y. Cai, W. Liu, C. Bao, J. Shen, Q. Liao, Estimating the state of health of lithium-ion batteries based on a probability density function, Int. J. Electrochem. Sci. 18 (6) (Jun. 2023) 100137, https://doi.org/10.1016/j.ijoes.2023.100137.
[36] P. Venugopal, et al., Analysis of optimal machine learning approach for battery life estimation of Li-ion cell, IEEE Access 9 (2021) 159616–159626, https://doi.org/10.1109/ACCESS.2021.3130994.
[37] P. Kumari, N. Kumar, Hybrid optimized deep learning approach for prediction of battery state of charge, state of health and state of temperature, Electrical Engineering 106 (2) (Apr. 2024) 1283–1290, https://doi.org/10.1007/s00202-023-02105-w.
[38] Y. Zheng, J. Hu, J. Chen, H. Deng, W. Hu, State of health estimation for lithium battery random charging process based on CNN-GRU method, Energy Rep. 9 (May 2023) 1–10, https://doi.org/10.1016/j.egyr.2022.12.093.
[39] V. Myilsamy, S. Sengan, R. Alroobaea, M. Alsafyani, State-of-Health prediction for Li-ion batteries for efficient battery management system using hybrid machine learning model, Journal of Electrical Engineering & Technology 19 (1) (Jan. 2024) 585–600, https://doi.org/10.1007/s42835-023-01564-2.
[40] H.S. Oh, J.M. Kim, C.Y. Chang, A study on LSTM-based lithium battery SoH estimation in urban railway vehicle operating environments, Journal of Electrical Engineering & Technology 19 (4) (May 2024) 2817–2829, https://doi.org/10.1007/s42835-024-01864-1.
[41] L. Ren, J. Dong, X. Wang, Z. Meng, L. Zhao, M.J. Deen, A data-driven auto-CNN-LSTM prediction model for lithium-ion battery remaining useful life, IEEE Trans Industr Inform 17 (5) (May 2021) 3478–3487, https://doi.org/10.1109/TII.2020.3008223.
[42] B. Zou, et al., A deep learning approach for state-of-health estimation of lithium-ion batteries based on a multi-feature and attention mechanism collaboration, Batteries 9 (6) (Jun. 2023) 329, https://doi.org/10.3390/batteries9060329.
[43] M. Lin, C. Yan, W. Wang, G. Dong, J. Meng, J. Wu, A data-driven approach for estimating state-of-health of lithium-ion batteries considering internal resistance, Energy 277 (Aug. 2023) 127675, https://doi.org/10.1016/j.energy.2023.127675.
[44] J. Xu, B. Liu, G. Zhang, J. Zhu, State-of-health estimation for lithium-ion batteries based on partial charging segment and stacking model fusion, Energy Sci. Eng. 11 (1) (Jan. 2023) 383–397, https://doi.org/10.1002/ese3.1338.
[45] Q. Gong, P. Wang, Z. Cheng, A data-driven model framework based on deep learning for estimating the states of lithium-ion batteries, J. Electrochem. Soc. 169 (3) (Mar. 2022) 030532, https://doi.org/10.1149/1945-7111/ac5bac.
[46] X. Hu, Y. Che, X. Lin, Z. Deng, Health prognosis for electric vehicle battery packs: a data-driven approach, IEEE ASME Trans. Mechatron. 25 (6) (Dec. 2020) 2622–2632, https://doi.org/10.1109/TMECH.2020.2986364.
[47] G. Yüksek, A. Alkaya, An Adaptive Energy Management Approach for Battery-Supercapacitor Hybrid Energy Storage System', Bulletin of the Polish Academy of Sciences Technical Sciences, Apr. 2024 https://doi.org/10.24425/bpasts.2024.150203, 150203–150203.
[48] G. Qi, N. Ma, K. Wang, Predicting the remaining useful life of supercapacitors under different operating conditions, Energies 17 (11) (May 2024) 2585, https://doi.org/10.3390/en17112585.
[49] A. Zahoor, R. Kun, G. Mao, F. Farkas, A. Sápi, Z. Kónya, Urgent needs for second life using and recycling design of wasted electric vehicles (EVs) lithium-ion battery: a scientometric analysis, Environ. Sci. Pollut. Control Ser. 31 (30) (Jun. 2024) 43152–43173, https://doi.org/10.1007/s11356-024-33979-3.
[50] Z. Zhou, B. Duan, Y. Kang, Q. Zhang, Y. Shang, C. Zhang, Online state of health estimation for series-connected $LiFePO_4$ battery pack based on differential voltage and inconsistency analysis, IEEE Transactions on Transportation Electrification 10 (1) (Mar. 2024) 989–998, https://doi.org/10.1109/TTE.2023.3274819.
[51] Y. Song, D. Liu, Y. Peng, Series-connected lithium-ion battery pack health modeling with cell inconsistency evaluation, in: 2019 IEEE International Instrumentation and Measurement Technology Conference (I2MTC), IEEE, May 2019, pp. 1–6, https://doi.org/10.1109/I2MTC.2019.8827097.
[52] Y. Che, et al., State of health prognostics for series battery packs: a universal deep learning method, Energy 238 (Jan. 2022) 121857, https://doi.org/10.1016/j.energy.2021.121857.
[53] P. Xu, et al., State of health estimation of LIB based on discharge section with multi-model combined, Heliyon 10 (4) (Feb. 2024) e25808, https://doi.org/10.1016/j.heliyon.2024.e25808.
[54] L. Lu, H. Zhai, Y. Gao, New energy electric vehicle battery health state prediction based on vibration signal characterization and clustering, Heliyon 10 (1) (Jan. 2024) e23420, https://doi.org/10.1016/j.heliyon.2023.e23420.
[55] W. Wang, et al., An end-cloud collaboration approach for online state-of-health estimation of lithium-ion batteries based on multi-feature and transformer, J. Power Sources 608 (Jul. 2024) 234669, https://doi.org/10.1016/j.jpowsour.2024.234669.
[56] A. Krizhevsky, I. Sutskever, G.E. Hinton, ImageNet classification with deep convolutional neural networks, in: Advances in Neural Information Processing Systems, vol. 25, 2012 [Online]. Available: http://code.google.com/p/cuda-convnet/.
[57] K. He, X. Zhang, S. Ren, J. Sun, Deep Residual Learning for Image Recognition, Dec. 2015.
[58] J. Redmon, A. Farhadi, YOLOv3: an Incremental Improvement, Apr. 2018.
[59] Y. Meyer, Wavelets and Operators, vol. 1, Cambridge University Press, 1993, https://doi.org/10.1017/CBO9780511623820.
[60] Christoph Robert Birkl, 'Oxford Battery Degradation Dataset 1', 2017.
[61] Y. Xing, E.W.M. Ma, K.-L. Tsui, M. Pecht, An ensemble model for predicting the remaining useful performance of lithium-ion batteries, Microelectron. Reliab. 53 (6) (Jun. 2013) 811–820, https://doi.org/10.1016/j.microrel.2012.12.003.
[62] M.K. Kıymık, İ. Güler, A. Dizibüyük, M. Akın, Comparison of STFT and wavelet transform methods in determining epileptic seizure activity in EEG signals for real-time application, Comput. Biol. Med. 35 (7) (Oct. 2005) 603–616, https://doi.org/10.1016/j.compbiomed.2004.05.001.
[63] J.M. Lilly, S.C. Olhede, Generalized Morse wavelets as a superfamily of analytic wavelets, IEEE Trans. Signal Process. 60 (11) (Nov. 2012) 6036–6041, https://doi.org/10.1109/TSP.2012.2210890.
[64] K. Schneider, M. Farge, Wavelets: mathematical theory, in: Encyclopedia of Mathematical Physics, Elsevier, 2006, pp. 426–438, https://doi.org/10.1016/B0-12-512666-2/00153-X.